Authors

Brittany A. Petros*[1,2,3,4], Jillian S. Paull*□[1,4], Christopher H. Tomkins-Tinch*□[1,5], Bryn C. Loftness*□[1,6,7,8], Katherine C. DeRuff[1], Parvathy Nair[1], Gabrielle L. Gionet[1], Aaron Benz[9], Taylor Brock-Fisher[1], Michael Hughes[10], Leonid Yurkovetskiy[11], Shandukani Mulaudzi[12], Emma Leenerman[10], Thomas Nyalile[11], Gage K. Moreno[1], Ivan Specht[1], Kian Sani[1], Gordon Adams[1], Simone V. Babet[13], Emily Baron[14], Jesse T. Blank[10], Chloe Boehm[1,15], Yolanda Botti-Lodovico[1], Jeremy Brown[10], Adam R. Buisker[10], Timothy Burcham[16], Lily Chylek[1], Paul Cronan[16], Valentine Desreumaux[13], Megan Doss[17], Belinda Flynn[10], Adrianne Gladden-Young[1], Olivia Glennon[16], Hunter D. Harmon[10], Thomas V. Hook[13], Anton Kary[18], Clay King[19], Christine Loreth[1], Libby Marrs[16], Kyle J. McQuade[18], Thorsen T. Milton[13], Jada M. Mulford[18], Kyle Oba[16], Leah Pearlman[1], Mark Schifferli[16], Madelyn J. Schmidt[10], Grace M. Tandus[13], Andy Tyler[10], Megan E. Vodzak[1], Kelly Krohn Bevill[6], Andres Colubri[1,20], Bronwyn L. MacInnis[1], A. Zeynep Ozsoy[18], Eric Parrie[14], Kari Sholtes[6,13], Katherine J. Siddle[1,5], Ben Fry[#16], Jeremy Luban[#1,11,21,22], Daniel J. Park[#1], John Marshall[#10], Amy Bronson[#23], Stephen F. Schaffner[#1], Pardis C. Sabeti[#1,5,22,24,25]

[1]Broad Institute of MIT and Harvard, Cambridge, MA, 02142, USA. [2]Harvard-MIT Program in Health Sciences and Technology, Cambridge, MA, 02139, USA. [3]Harvard/MIT MD-PhD Program, Boston, MA, 02115, USA. [4]Systems, Synthetic, and Quantitative Biology PhD Program, Department of Systems Biology, Harvard Medical School, Boston, MA, 02115, USA. [5]Department of Organismic and Evolutionary Biology, Harvard University, Cambridge, MA, 02138, USA. [6]Department of Computer Science and Engineering, Colorado Mesa University, Grand Junction, CO, 81501, USA. [7]Complex Systems and Data Science PhD Program, University of Vermont, Burlington, VT, 05405, USA. [8]Vermont Complex Systems Center, University of Vermont, Burlington, VT, 05405, USA. [9]Degree Analytics, Inc., 1905 Kramer Lane Suite A100, Austin, TX, 78758, USA. [10]Colorado Mesa University, Grand Junction, CO, 81501, USA. [11]Program in Molecular Medicine, University of Massachusetts Chan Medical School, Worcester, MA, 01655, USA. [12]Harvard Program in Bioinformatics and Integrative Genomics, Harvard Medical School, Boston, MA, 02115, USA. [13]Department of Civil, Environmental, and Architectural Engineering, University of Colorado, Boulder, CO, 80309, USA. [14]COVIDCheck Colorado, LLC., Denver, CO, 80202, USA. [15]Princeton University Molecular Biology Department, Princeton, NJ, 08544, USA. [16]Fathom Information Design, Boston, MA, 02114, USA. [17]Warrior Diagnostics, Inc., Loveland, CO, 80538, USA. [18]Department of Biological Sciences, Colorado Mesa University, Grand Junction, CO, 81501, USA. [19]Department of Mathematics and Statistics, Colorado Mesa University, Grand Junction, CO, 81501, USA. [20]University of Massachusetts Medical School, Worcester, MA, 01655, USA. [21]Biochemistry and Molecular Pharmacology, University of Massachusetts Medical School, Worcester, MA, 01655, USA. [22]Massachusetts Consortium on Pathogen Readiness, Boston, MA, 02115, USA. [23]Physician Assistant Program, Department of Kinesiology, Colorado Mesa University, Grand Junction, CO, 81501, USA. [24]Department of Epidemiology, Harvard T.H. Chan School of Public Health, Boston, MA, 02115, USA. [25]Howard Hughes Medical Institute, Chevy Chase, MD, 20815, USA.

*, these authors contributed equally.

□, corresponding authors: tomkinsc@broadinstitute.org (lead contact); jpaull@broadinstitute.org (wastewater); bloftnes@broadinstitute.org (wifi).

[#], these authors jointly supervised this work.

Title

Multimodal surveillance of SARS-CoV-2 at a university enables development of a robust outbreak response framework

Abstract

Universities are particularly vulnerable to infectious disease outbreaks and are also ideal environments to study transmission dynamics and evaluate mitigation and surveillance measures when outbreaks occur. Here, we introduce a SARS-CoV-2 surveillance and response framework based on high-resolution, multimodal data collected during the 2020-2021 academic year at Colorado Mesa University. We analyzed epidemiological and sociobehavioral data (demographics, contact tracing, and wifi-based co-location data) alongside pathogen surveillance data (wastewater, random, and reflexive diagnostic testing; and viral genomic sequencing of wastewater and clinical specimens) to characterize outbreak dynamics and inform policy decisions. We quantified group attributes that increased disease risk, and highlighted parallels between traditional and wifi-based contact tracing. We additionally used clinical and environmental viral sequencing to identify cryptic transmission, cluster overdispersion, and novel lineages or mutations. Ultimately, we used distinct data types to identify information that may help shape institutional policy and to develop a model of pathogen surveillance suitable for the future of outbreak preparedness.

Intro

Infectious disease outbreaks are existential threats to congregate communities; in universities, in particular, students are susceptible because of close-quarters housing[1,2], dense social networks[3–5], and widespread involvement in sports teams and other student organizations[5,6]. Students may also be individually vulnerable to infection due to sleep deprivation[7] and poor hygiene[8]. In addition to their own susceptibility, universities have potential to drive transmission in surrounding communities[9–11].

At the same time, residential universities are ideal environments for the study of pathogen transmission and the impact of interventions and surveillance thanks to their semi-insular character and their role as centers of innovation[12]. In response to SARS-CoV-2 they have widely employed high-cadence testing[13–15], vaccination programs[16,17], strict quarantine of cases in dedicated facilities[18–21], and social distancing measures[22–25]. In addition, universities are well-positioned to test and implement new surveillance methods that can subsequently be applied at greater scale. For example, they were among the first to implement wastewater surveillance for SARS-CoV-2[18,26], institution-wide viral sequencing[21,27], and contact tracing via wifi network co-location data[28,29].

In Fall 2020, Colorado Mesa University (CMU) committed to in-person instruction of ~8,000 students for the 2020–2021 academic year, motivated by a desire to avoid amplifying resource disparities via remote learning. This decision necessitated a rigorous SARS-CoV-2 surveillance program, balancing public health goals with efficient use of limited resources. Given these considerations, CMU eschewed mandatory periodic testing of all university community members in favor of a surveillance program with randomized testing and robust reflexive testing – *i.e.*, strategic testing of students due to symptoms (reported through the *Scout* web-based tool[30]), contact with recently diagnosed individuals, or a positive wastewater signal in their residential dorm.

CMU piloted *Lookout*, a tool integrating multiple data types to identify, alert, and test individuals or groups at increased risk of infection (Figure 1; demo: https://sentinel.network/lookout-demo-campus). Lookout integrated numerous data types, including clinical diagnostic test results, student attributes such as residence hall and sports team affiliations, self-reported contacts of positive individuals, viral genome sequences from diagnostic specimens, and wastewater viral titers. The interactive dashboard allowed the administration to quickly identify students at risk of infection and to minimize opportunities for transmission. Here, we explore the utility of combining these and additional data types (including wifi co-location logs and genome sequences from wastewater effluent) to design effective disease surveillance systems.

Results

1. CMU deployed a comprehensive and effective surveillance program based on a multi-pronged testing approach

Over the 2020–2021 academic year, CMU's surveillance program identified 1,113 COVID-19 cases (1,076 students, 37 faculty or staff) through randomized and targeted (*i.e.*, symptomatic or reflexive) testing. The test positivity rate was 5.1% in Fall 2020 (August 17–November 20) and 1.5% in Spring 2021 (January 18–April 30) (Figure 2A–C); individuals who tested positive were moved to an isolation dorm. CMU's randomized testing strategy sampled students non-uniformly to test more frequently those at greater risk of onward transmission, *i.e.*, on-campus students and athletes. Consistent with this bias, on-campus students and athletes ultimately tested positive 1.30 and 2.45 times as frequently as expected given uniform sampling (Appendix Figure 1C).

In addition, CMU's reflexive testing program tested individuals identified by institutional contact tracing as close contacts. Of the identified positive individuals, 720 (65%) reported close contacts, enabling subsequent detection of 93 distinct cases (8.4% of the total cases) within a week of the sentinel case's positive test. These efforts identified plausible transmission links; among pairs of sequenced cases identified via contact tracing, 79% had closely related genomes (with a genetic distance of at most two mutations), compared to 10% among sequenced pairs more generally (Appendix Figure 2A).

Frequent wastewater surveillance enhanced reflexive testing efforts, identifying SARS-CoV-2-positive residence halls whose residents were then randomly selected for follow-up testing. The effort captured effluent from ~75% (Fall) and ~85% (Spring) of the residential student population. In response to spikes in viral titer, contributing residence halls were oversampled for testing; when warranted, up to half of the residents of a hall were tested. The success of this program is reflected in the close correlation of wastewater viral titer with contemporaneous case counts (Spearman ρ=0.40, $p<.001$; Figure 5AB, Appendix Figure 3).

To assess the overall efficacy of CMU's surveillance program, we compared CMU's incidence rate to that of Mesa County, which had limited testing available at the time. CMU's weekly

incidence exceeded county incidence rates and predicted them with a lag time of 3 days (correlation = 0.73; Appendix Figure 1AB). This is consistent with reports that adequate university testing can foreshadow community outcomes[12] and highlights the ability of well-designed university testing programs to serve as bellwethers. As the pandemic's impact on the surrounding community became clearer, the university sponsored testing for external community members, both as a public benefit and to limit spread of SARS-CoV-2 into the campus[31].

2. Epidemiological analyses identified student attributes associated with SARS-CoV-2 positivity and support a surveillance paradigm of targeted testing and risk mitigation

Here we evaluate risk factors among a wide range of institutionally captured attributes for individuals who tested positive: role (*i.e.*, student or faculty/staff), sex, class year[32], test date, association with a residence hall, and membership in a sports team. Residence halls (Appendix Table 1) and sports teams (Appendix Table 2) were annotated with features, including perceived contact risk for sports teams (defined in Appendix Table 3). Our results support a two-pronged surveillance strategy, in which groups at increased risk are targeted for higher-cadence testing, while putatively causal factors are mitigated via institutional policies that reduce risk.

Besides athletes and on-campus students, whose higher risk of testing positive could reflect increased sampling, males, freshmen, and juniors also exhibited more cases than expected by chance (Appendix Figure 1C; Figure 2E; Appendix Table 4). These findings may underscore risk factors relevant for other universities: for example, a potential commonality between freshmen and juniors is that many students moved to new living arrangements (on-campus for freshmen, off-campus for juniors). Future surveillance efforts could target populations undergoing such transitions, though real-time epidemiology is essential to identify community-specific risk factors.

Looking more closely among sports teams, we identified specific attributes that further predict disease risk. High-contact sports teams had increased disease risk (Appendix Table 4), with 50% more cases than expected from the risk for athletes as a whole, while low-contact teams had 47% fewer. Interestingly, risk was not uniform across teams of comparable contact level; women's basketball had 90% more cases than expected, while men's soccer had 16% fewer, despite both being high-contact sports (Figure 2D). We found no association between sports location (*i.e.*, indoor *vs.* outdoor sports) and case counts, though sports played in both seasons had higher case incidence than fall or spring sports (Appendix Table 4). These findings are consistent with a model where individual athletes sporadically contract COVID-19, with an increased risk of further transmission and thus outbreaks on higher-contact teams or teams with longer seasons.

Because COVID-19 incidence rates varied approximately three-fold from 9.7% to 27% across residence halls (Appendix Table 1), we conducted linear regression with multiple possible predictors related to halls to characterize factors that influenced case rates (Appendix Figure 4AB). Two features were significant predictors: percent occupancy (*i.e.*, number of available

beds filled) and private (*vs.* hallway) bathrooms (see Appendix Figure 4C-E for model validation). We included an indicator variable for fall wastewater tracking to assess whether reflexive testing biased hall incidence rates; it was dropped as a predictor and thus does not significantly bias rates.

For every increase of 10% in occupancy, our model predicted an increase of 0.015 in incidence, supporting institutional de-densification measures to limit the transmission risks associated with denser populations. Strikingly, halls with en-suite or private bathrooms were predicted to have an incidence 0.059 higher than those with hallway bathrooms (Appendix Figure 4B), consistent with reports that a majority of SARS-CoV-2 transmissions occur within households (here, within suites)[33]. Possible explanations include compensatory protective measures (*i.e.*, masking or social distancing) present in larger bathrooms and the increased hygiene of hallway bathrooms, which were cleaned by professional staff rather than residents. Importantly, our model does not account for possible social confounders such as clustering of certain groups (*e.g.*, athletes or freshmen) within specific residence halls.

3. Distinct interaction dynamics of positive individuals within wifi proximity dataset reveal potential for incorporation into disease surveillance

Here, we explore a dataset of anonymized daily logged connection locations (*i.e.*, access point and building) for students connected to campus wifi for at least 15 minutes, and describe how such data can be extended for real-time disease surveillance. Data were obtained from an existing program implemented in 2018 to assess facility use and student engagement, in order to aid the university in allocation of resources. All students were alerted via a campus-wide notice about the program, and could choose to opt out; an overwhelming majority (98%) participated.

Through an examination of campus-wide connectivity patterns, we identified associations between student activity and CMU's COVID-19-related policies. We found elevated on-campus presence during weekdays (*vs.* weekends) and in residence halls (*vs.* other building types) in fall 2020 (Appendix Figures 5, 6A, 6C), reflecting university policies that discouraged on-campus gathering. When mitigation policies relaxed in Spring 2021, weekend presence increased relative to fall 2020 (Appendix Figure 6B and 6D). Additionally, after testing positive, individuals had 42% fewer contacts than during the preceding 10 days, indicating adherence to isolation policies (Appendix Figure 7A). This quantification of policy adherence suggests that wifi datasets can be used to assess policy implementation or to determine the effects of policy updates in real time.

We found that positive individuals exhibited distinct patterns in their social networks and behaviors. Individuals who eventually tested positive exhibited larger social networks than those who remained negative: they spent more days on campus (Appendix Figure 7B), had more daily contacts (Figure 3A, left), and interacted for a longer duration with each contact (Figure 3A, right), creating more opportunities for potential viral transmission. Furthermore, in the 10 days preceding both of their positive tests, pairs of students identified *via* contact tracing had significantly longer daily interaction times than other pairs of positive students (*e.g.*, median of

104 *vs.* 45 minutes per interaction per day in the fall; Appendix Figure 7CD). Moreover, these pairs of positive students between whom COVID-19 transmission may have occurred interacted for significantly longer than for pairs in which transmission did not or could not have occurred (*i.e.*, pairs involving one or more students who never tested positive; Appendix Figure 7CD). These distinct qualities support supplementing, and if necessary substituting, manual contact tracing with a wifi-based system to automatically flag close contacts of positive individuals.

We further explored interactions between positive and negative individuals using the attribute assortativity metric (AA), which quantifies the extent to which individuals interact within-group *vs.* between-group compared to random assortment (Figure 3B). We found that both positive (*i.e.*, individuals positive at any point over the semester) and pre-positive individuals (*i.e.*, individuals within 10 days of a positive test) were more likely to associate with one another than with negative individuals (Figure 3C, Appendix Figure 8A–C). Importantly, this relationship remained significant, albeit with a lower effect size, when removing pre-positive individuals who identified one another as close contacts, suggesting that this finding is not limited to positive individuals identified via reflexive testing secondary to manual contact tracing (Appendix Figure 9). Interestingly, the AA for pre-positive individuals was a leading indicator of daily case counts, by 8 days (Fall) and 3 days (Spring; Figure 3DE, Appendix Figure 8D–F), suggesting that the degree of within-group interactions among putatively infectious individuals increases in the days leading to these individuals' positive tests.

4. Phylogenetic analysis of clinical viral genomes identified cluster size overdispersion and cryptic transmissions, leading to concrete policy decisions

Viral genomic sequencing from residual biomaterial enables exploration of transmission dynamics and rapid detection and monitoring of SARS-CoV-2 variants. At CMU, sequencing facilitated detection of 18 distinct Pango lineages (Figure 4A; Appendix Figure 2BC)[34]. Of these, B.1.2 was the most abundant both at CMU and in Colorado, reflecting circulation between CMU and the surrounding community and highlighting the importance of CMU's sponsored testing for Mesa County[35]. We identified continuous transmission of this lineage between semesters, with 7 spring cases descending from 17 fall cases as the likely result of 2–3 cryptic intermediate transmissions during winter recess[36]. This cluster was non-significantly enriched for off-campus students relative to the remaining sequenced cases (83% *vs.* 70% off-campus; $p = 0.15$); possible off-campus continuation of the transmission chain over the break suggests that institutional surveillance programs would be wise to maintain testing availability for nearby students during school breaks.

We detected overdispersion in both genomic and social clustering data, highlighting the importance of policies that minimize super-spreading events. Of 41 detected introductions to the university, onward transmission was only observed from 13, with 5 of the resulting clusters containing 80% of sequenced cases ($k=0.12$ in a negative binomial model, consistent with other studies[37,38]; Figure 4BC). We also observed overdispersion in the number of contacts between individuals in both contact tracing and wifi proximity analyses, where 80% of reported contacts were made by 33% ($k=0.83$) and 43% ($k=0.89$) of positive individuals, respectively (Figure 4DE). The similar shape of these contact distributions suggests that both datasets capture the

true underlying structure of social interactions. Notably, phylogenomic cluster size demonstrates greater overdispersion than the two contact count distributions, suggesting that overdispersion in SARS-CoV-2 transmission can be partitioned into both social and biological components. Given the high variance observed amongst all three distributions, we suggest that both biological and social factors influence large SARS-CoV-2 case clusters, and that their interplay warrants further investigation. Below, we investigate the impact of a variety of variables on a distinct spring cluster.

5. Contemporaneous wastewater viral sequencing supplements lineage detection and enables detection of emergent mutations

During 6 weeks from February to mid-March 2021, we obtained 42 wastewater samples from 10 sites for sequencing, 9 of which were sequenced in duplicate (Appendix Figure 3C). The concurrent collection of wastewater samples and clinical specimens, with high breadth of coverage among the residential population, allowed us to directly compare viral sequences from wastewater with those from contemporaneous individual cases. Through this, we validated the utility of wastewater viral sequencing as a component of a comprehensive pathogen surveillance program, as currently instantiated by *Lookout*.

As expected, wastewater viral titers were lower than titers of clinical specimens collected from upstream individuals (Appendix Figure 10A). Wastewater and clinical samples from CMU had similar sequence coverage, suggesting that there was no particular bias in viral RNA degradation in wastewater (Appendix Figure 10B–E). This demonstrates that these wastewater samples were comparable to clinical specimens in integrity and suitable for sequencing and genomic surveillance.

We used the pre-existing Freyja tool[39,40] to detect 8 lineages in wastewater, 3 of which were found in concurrent clinical cases (Figure 5C, Appendix Table 6). Another 3 were observed in clinical cases prior to wastewater collection, suggesting undetected circulation on campus, shedding from previously-infected individuals, or environmental persistence. The remaining 2, B.1.533 and B.1.350, were present in the US but not the campus or state[35]; each was detected at low abundance in single samples and likely originated from a small number of individuals. Wastewater sequencing thus identified lineages not concurrently detected via clinical sequencing, proving itself to be particularly relevant in instances of incomplete clinical genomic sampling.

In addition to detection of defined lineages, wastewater sequencing can also identify novel mutations; for this latter use case, we found that quality control mechanisms were essential to identify true variation. Of 1521 wastewater single nucleotide variants (SNVs), 85% and 68% were not found at consensus-level in CMU and Colorado clinical samples, respectively, and only 4% were derived from clinical minor alleles (Figure 5D). We thus hypothesized that many mutations arose from amplification errors (*e.g.*, formation of chimeras), a theory supported by the order-of-magnitude difference in the number of SNVs detected in wastewater *vs*. clinical samples as a function of sample count (Appendix Figure 11). We subsequently developed quality control methods to corroborate mutations *via* detection in state-wide clinical genomes.

We achieved high specificity for discarding SNVs not seen in Colorado when we required presence in both of two technical replicates (specificity = 98%) or an allele frequency exceeding 25% (specificity = 92%); both methods had low sensitivity (50% and 62%, respectively; Figure 5E), as each excluded SNVs corroborated by clinical viral genomes. This analysis provides real-word evidence of the importance of replicates for identifying true SNVs in wastewater samples, a finding previously shown for clinical minor allele validation[41].

Of 68 replicate-corroborated SNVs found across 9 wastewater samples with 2 technical replicates, 11 (16%) were not seen in clinical CMU samples (Appendix Table 7). 6 of the 11 were present in Colorado and had allele frequencies >96% in single wastewater specimens, likely reflecting on-campus circulation of viral genotypes unsampled by clinical sequencing. Of the 5 remaining mutations, 2 were non-synonymous mutations in ORF1ab (I1970S, T3462I) and were novel compared with published global variation[35], 2 were synonymous mutations, and 1 was a premature stop codon. The latter mutation, with an allele frequency of 4%, may be spurious; the other 4, with allele frequencies between 27% and 100%, could reflect either gut tropism or cryptic transmission. Though these mutations' phenotypic effects remain unknown, their identification serves as a proof-of-concept and provides a framework for detection of novel mutations in wastewater.

6. Detection of novel lineage B.1.429.1 on campus leads to high-resolution characterization of social and biological factors implicated in its spread

In Spring 2021, we detected a cluster of cases on campus that was concerning due to its unprecedented size and genomic ancestry, and proceeded to characterize it analytically and experimentally to identify the social and biological factors that contributed to its rise. This B.1.429.1 cluster initiated as a single introduction to campus, which proliferated into several star-like descendant sub-clusters, consistent with clonal amplification (Figure 6A). In total, the outbreak lasted for 45 days; in its final 4 weeks, it represented 33% of sequenced clinical samples and was the most abundant lineage in 47% of wastewater samples (Figure 6AB). B.1.429.1 descended from B.1.429 – then deemed a Variant of Concern due to reduced antibody neutralization and increased viral shedding, infectivity, and transmissibility[42] – but also included the recurrent S:Q677H substitution, posited to further increase transmissibility[43] (Appendix Table 8).

We did not detect differences in interaction patterns among individuals with B.1.429.1 *vs.* those with other viral lineages (Appendix Figure 12AB), suggesting that its transmissibility was due to inherent qualities of the lineage rather than the specific social dynamics of the individuals within the cluster. We did find that these individuals clustered together in social networks (Figure 6C); *i.e.*, they were on average one social connection closer to one another than to other positive individuals ($p<0.001$). Wifi-connected B.1.429.1 pairs also had significantly lower genetic distances between their viral genomes than non-connected B.1.429.1 pairs (Figure 6D), demonstrating that connections observed within the wifi network are enriched for genuine transmission events.

We inferred direct transmission links among B.1.429.1 cases and found that wifi connectivity data inferred transmission networks that paralleled those constructed following traditional contact tracing. Alone, manual contact tracing or genomic sequencing resolved transmission links for 61% and 68% of individuals, respectively (Appendix Figure 12DE). We thus combined genomic data with traditional contact (2 days prior to tests) or wifi-derived contract tracing (for both 2 and 10 days prior to tests), producing transmission models connecting 82%, 87%, and 74% of sequenced cases, respectively (Figure 6EF, Appendix Figure 12F). We compared the cluster topology for these networks and found that the wifi 10-day data best approximated the traditional contact tracing network (*via* Jaccard distance; Appendix Table 10). Due to the paucity of distinguishing mutations present between individual consensus mutations[44], we used intrahost viral variation to supplement our transmission linkages. We identified a clear transmission chain where a single mutation present at low frequency in one specimen (#26 in Figure 6EF) reached fixation in two specimens (#27 & 28 in Figure 6EF) collected one week later, consistent with bottlenecked transmission. These three individuals clustered together in all reconstruction networks, but without the directionality of transmission inferred from minor alleles or phylogenetic descent, implying that transmission network reconstruction tools would benefit from further refinement.

We next analyzed inherent phenotypic factors that could explain the increased transmission of B.1.429.1 on campus. We assessed the impact of the S:Q677H mutation found in B.1.429.1 on single-cycle infectivity and on cell-to-cell fusogenicity in lentiviral pseudotypes (Appendix Figure 12GH). While the mutation did not alter virion spike protein levels or cell-free virion infectivity (Appendix Figure 12C), it significantly increased fusion efficiency relative to the ancestral B.1.429 spike protein (Figure 6G), likely due to proximity to the spike protein polybasic cleavage site. We found similar results for the S:Q677P mutation, which was detected in other contemporaneous CMU lineages. This finding is consistent with greater within-host dissemination of SARS-CoV-2 haplotypes bearing S:Q677H or S:Q677P.

Fortunately, B.1.429.1 was minimally detected outside the campus, pointing to the success of CMU's containment policies. This vignette highlights the power of systematic, multimodal surveillance programs to not only identify and mitigate transmission events, but also to contribute to novel biological characterization of viral lineages.

Discussion

In this paper, we analyzed clinical diagnostic data, case attributes, wifi co-location logs, wastewater samples, and viral genomic sequences to quantify the success of CMU's pandemic response program and to assess the relevance of each data type for infectious disease surveillance. Our analyses showed that through contact tracing, wastewater surveillance, and increased focus on high-risk groups, CMU effectively identified positive cases. Via novel analyses of wifi connectivity, we confirmed adherence to school policies and evaluated metrics that could allow wifi data to replace or supplement traditional contact tracing.

In addition, we leveraged phylogenetic and epidemiological analyses to propose future policies to limit disease spread (*e.g.*, continued testing during school breaks, community testing, risk

prediction for testing prioritization) and to identify and mitigate specific causal factors shown to increase risk (*e.g.*, requiring high-quality masking or increased testing to participate in high-contact sports). Our sequencing of extant wastewater samples not only identified lineages independently of clinical sequencing, but also led us to apply and verify methodological procedures necessary for the detection of novel mutations from wastewater. Finally, through analysis of case cluster overdispersion and the novel lineage B.1.429.1, we highlighted the relevance of investigating both virological and sociobehavioral factors that can influence transmission.

Our results lead us to formulate a framework combining the analyzed tools within an integrated disease surveillance system (described in Figure 7). First, we emphasize beginning with mitigation policies such as symptom reporting, contact tracing, and quarantine and continuing with efficient testing strategies such as wastewater surveillance. While contact tracing is essential, it is also time-intensive and expensive to maintain; with further work to address technological and privacy concerns, wifi proximity and geolocation data could supplement and perhaps ultimately replace these efforts. Gathering epidemiological metadata, symptom attestations, and diagnostic test results digitally and with programmatic synthesis is also a high priority because it can facilitate real-time analyses and subsequent policy adjustments; the *Lookout* system serves as a useful template (Figure 1)[30]. If finances allow, we would add genomic surveillance to aid identification of transmission patterns and concerning lineages or mutations. For communities with wastewater surveillance, sequencing these samples provides a cheaper alternative to clinical sequencing of all upstream individuals and still allows for identification of lineages or mutations of interest. This tool cannot wholly replace clinical sequencing due to its inability to discern transmission trends. It is important to emphasize that disease surveillance is not a one-size-fits-all endeavor; in fact, we found parallel results across data types. We suggest that automated integration of a subset of data types will more powerfully combat infectious disease outbreaks than a siloed implementation of all data types.

Our findings are subject to statistical, methodological, and policy-based limitations. As with all studies of infectious disease surveillance, transmission events and clustering can violate statistical assumptions of independence among individuals. Additionally, while CMU had access to attribute data for individuals who never tested positive in the *Lookout* system, we were unable to access it for research under our existing regulatory approval; this impeded our ability to separate the impact that individual attributes (*e.g.*, a particular sports team or residence hall) had on risk of infection. Moreover, incomplete sampling of residual diagnostic biospecimen and wastewater samples limited us to a partial snapshot of SARS-CoV-2 genetic diversity at CMU (Figure 2A; Appendix Figure 3C). Further, wifi co-location logs remain an underexplored data source that does not capture off-campus interactions and likely records superfluous or false interactions. As our study largely took place prior to the widespread availability of SARS-CoV-2 vaccines[45] and of rapid at-home antigen tests[46], we cannot assess their impact on infectious disease transmission or policy. Finally, CMU's surveillance paradigm prioritized community safety over individual privacy; thus, some of our findings may not be generalizable to institutions with different prioritizations.

Accounting for resource constraints, we built upon CMU's community-driven mindset to develop an efficient surveillance program and lay the groundwork for future advances. While a number of analyses here were conducted only retrospectively, updates to surveillance software like *Lookout*[30] could enable timely identification of risk factors for infection and spread, proximity and location patterns, and lineages or mutations that are rising in frequency or that have been categorized as Variants of Concern. They could further refine the accuracy of outbreak reconstruction by incorporating genomic data including major and minor alleles, and contact tracing obtained from manual efforts or wifi analyses, with reported contacts weighted by the length or nature of the interaction. In summary, we propose the seamless, automated integration of multiple data types as the most powerful way to combat infectious disease outbreaks as they unfold.

Methods

Code associated with the analyses of this study is available at: https://github.com/broadinstitute/sc2-cmu-study. Detailed methods are included in an appendix.

We identified factors associated with testing positive for SARS-CoV-2 *via* calculation of 1) relative risk for athletic participation, campus residency, and sex, and 2) Pearson's chi-square test for distinct sports teams, residence halls, and class years. We also fit a linear model to residence hall incidence rates as a function of various binary and continuous attributes of the buildings (Appendix Figure 4A).

We examined differences in daily wifi connectivity patterns between subgroups defined by infection status or viral lineage and quantified differences in relevant metrics (Appendix Table 11) across subgroups via the Mann-Whitney U test. We calculated attribute assortativity (AA) to assess the tendency of individuals to associate with in-group *vs.* across groups, and determined the lag time that maximizes the correlation between AA and case count.

We constructed a network of known positive individuals, and connected pairs of individuals with interactions within 10 days of both positive tests. We compared wifi network path distances (i.e cumulative number of edges on the shortest path connecting two individuals in the network) between individuals in each pair where both were infected with B.1.429.1 lineage virus against pairs where only one individual had this viral lineage. We next compared viral genome distances (i.e., number of SNVs) within pairs of individuals infected with B.1.429.1 lineage virus that were connected by a path in the network *vs.* not connected.

Rolling 24-hour wastewater aliquots were collected from sewer sites to (1) monitor SARS-CoV-2 concentration via RT-qPCR and (2) provide source material for viral genomic sequencing. Across all collection sites, we compared weekly case counts from source buildings against daily and weekly wastewater viral titers (via Spearman correlation and Fisher's exact test, respectively).

Excess material from clinical diagnostic tests and wastewater aliquots was sequenced following enrichment via PCR with ARTICv3-tiled amplicons.

LoFreq was used to call major and minor alleles within wastewater samples. Several quality control metrics were considered to discard spurious variation: minimum allele frequency, local sequencing depth, and concordance in variation across replicates[47]. Freyja was used to identify and estimate the abundance of constituent SARS-CoV-2 lineages[39]. We determined the average number of unique SNVs that a single additional sequenced sample contributes to a set of a given number of samples, via bootstrapping of distinct subsets of clinical or wastewater samples.

Clinical genomes were assembled using the Broad Institute viral-ngs pipelines and Nextstrain pipelines and assigned Pango lineages[34,48]. Genomes were placed in the phylogenetic context of genomes from cases outside the university community, weighted toward genomes from Colorado and surrounding states. Case clusters were identified based on a state change from not university-associated to university-associated, following ancestral state reconstruction of internal tree nodes.

Negative binomial distributions were fit to distributions of cluster size, the number of contacts in the wifi data set, and the number of contacts in the standard contact tracing data set. Contacts were defined as any interaction >15 minutes in the 48-hour period prior to testing or symptom onset.

Transmission networks were inferred using sequenced viral genomes and contact data using *outbreaker2*[49].

Lentiviral pseudotype assays were performed to assess the functional implications of the S:Q677H substitution on infectivity and fusogenicity.

Funding Acknowledgments

This work was supported by the National Science Foundation (NSF) Graduate Research Fellowship Program to J.S.P. (grant number 1745303), and C.H.T-T. (grant number 1745303); the Hertz Foundation to J.S.P.; the National Institute of General Medical Sciences to B.A.P. (grant number T32GM007753); the National Science Foundation (NSF) to B.C.L. (grant number 2046440); the Moore Foundation to B.C.L., the National Institute of Allergy and Infectious Diseases to B.C.L. (grant number 2U19AI110818) and to P.C.S. (grant number U19AI110818 and U01AI151812); the National Institutes of Health to J.L. (grant numbers R37AI147868 and R01AI148784); the Massachusetts Consortium on Pathogen Readiness to J.L.; the Centers for Disease Control and Prevention (CDC) COVID-19 baseline genomic surveillance contract to the Clinical Research Sequencing Platform (grant number 75D30121C10501) and a CDC Broad Agency Announcement to B.L.M. (grant number 75D30120C09605); and the Howard Hughes Medical Institute to P.C.S. This work was made possible by support from the Flu laboratory and a cohort of generous donors through TED's Audacious Project, including the ELMA Foundation, MacKenzie Scott, Skoll Foundation and Open Philanthropy.

Any opinion, findings, and conclusions or recommendations expressed in this material are those of the author(s) and do not necessarily reflect the views of the National Science Foundation. This content is solely the responsibility of the authors and does not necessarily represent the

official views of the National Institute of General Medical Sciences or the National Institutes of Health.

Acknowledgements

The authors wish to thank Jacob E. Lemieux for helpful discussions and feedback. The authors also wish to thank Laurent Hébert-Dufresne for providing insights and feedback on the wifi co-location analyses.

Conflicts of Interest

P.C.S. is a co-founder of, shareholder in, and scientific advisor to Sherlock Biosciences, Inc; she is also a Board member of and shareholder in Danaher Corporation. P.C.S. has filed IP related to genome sequencing and analysis.

Ethics Statement

The study was conducted at the Broad Institute with approval from the MIT Institutional Review Board under Protocol #1612793224 and from WCG IRB Protocol #20210166 under Protocol: Investigating Viral Emergence and Spread in Community Settings.

References

1. Shah, M., Quinlisk, P., Weigel, A., Riley, J., James, L., Patterson, J., Hickman, C., Rota, P.A., Stewart, R., Clemmons, N., et al. (2018). Mumps Outbreak in a Highly Vaccinated University-Affiliated Setting Before and After a Measles-Mumps-Rubella Vaccination Campaign-Iowa, July 2015-May 2016. Clin. Infect. Dis. *66*, 81–88.

2. Harrison, L.H., Dwyer, D.M., Maples, C.T., and Billmann, L. (1999). Risk of meningococcal infection in college students. JAMA *281*, 1906–1910.

3. Delbos, V., Lemée, L., Bénichou, J., Berthelot, G., Taha, M.-K., Caron, F., and B14 STOP study group (2013). Meningococcal carriage during a clonal meningococcal B outbreak in France. Eur. J. Clin. Microbiol. Infect. Dis. *32*, 1451–1459.

4. MacLennan, J., Kafatos, G., Neal, K., Andrews, N., Cameron, J.C., Roberts, R., Evans, M.R., Cann, K., Baxter, D.N., Maiden, M.C.J., et al. (2006). Social behavior and meningococcal carriage in British teenagers. Emerg. Infect. Dis. *12*, 950–957.

5. Segaloff, H.E., Cole, D., Rosenblum, H.G., Lee, C.C., Morgan, C.N., Remington, P., Pitts, C., Kelly, P., Baggott, J., Bateman, A., et al. (2021). Risk Factors for Severe Acute Respiratory Syndrome Coronavirus 2 (SARS-CoV-2) Infection and Presence of Anti-SARS-CoV-2 Antibodies Among University Student Dormitory Residents, September-November 2020. Open Forum Infect Dis *8*, ofab405.

6. Vang, K.E., Krow-Lucal, E.R., James, A.E., Cima, M.J., Kothari, A., Zohoori, N., Porter, A., and Campbell, E.M. (2021). Participation in Fraternity and Sorority Activities and the Spread of COVID-19 Among Residential University Communities - Arkansas, August 21-September 5, 2020. MMWR Morb. Mortal. Wkly. Rep. *70*, 20–23.

7. Nolan, T., O'Ryan, M., Wassil, J., Abitbol, V., and Dull, P. (2015). Vaccination with a multicomponent meningococcal B vaccine in prevention of disease in adolescents and young adults. Vaccine *33*, 4437–4445.

8. Prater, K.J., Fortuna, C.A., McGill, J.L., Brandeberry, M.S., Stone, A.R., and Lu, X. (2016). Poor hand hygiene by college students linked to more occurrences of infectious diseases, medical visits, and absence from classes. Am. J. Infect. Control *44*, 66–70.

9. Lu, H., Weintz, C., Pace, J., Indana, D., Linka, K., and Kuhl, E. (2021). Are college campuses superspreaders? A data-driven modeling study. Comput. Methods Biomech. Biomed. Engin. *24*, 1136–1145.

10. Valesano, A.L., Fitzsimmons, W.J., Blair, C.N., Woods, R.J., Gilbert, J., Rudnik, D., Mortenson, L., Friedrich, T.C., O'Connor, D.H., MacCannell, D.R., et al. (2021). SARS-CoV-2 Genomic Surveillance Reveals Little Spread From a Large University Campus to the Surrounding Community. Open Forum Infect Dis *8*, ofab518.

11. Crowe, J., Schnaubelt, A.T., Schmidt-Bonne, S., Angell, K., Bai, J., Eske, T., Nicklin, M., Pratt, C., White, B., Crotts-Hannibal, B., et al. (2021). Pilot program for test-based SARS-CoV-2 screening and environmental monitoring in an urban public school district. bioRxiv.

12. Petros, B.A., Turcinovic, J., Welch, N.L., White, L.F., Kolaczyk, E.D., Bauer, M.R., Cleary, M., Dobbins, S.T., Doucette-Stamm, L., Gore, M., et al. (2022). Early introduction and rise of the Omicron SARS-CoV-2 variant in highly vaccinated university populations. Clin. Infect. Dis.

13. Rennert, L., and McMahan, C. (2021). Risk of Severe Acute Respiratory Syndrome Coronavirus 2 (SARS-CoV-2) Reinfection in a University Student Population. Clin. Infect. Dis.

14. Paltiel, A.D., Zheng, A., and Walensky, R.P. (2020). Assessment of SARS-CoV-2 Screening Strategies to Permit the Safe Reopening of College Campuses in the United States. JAMA Netw Open *3*, e2016818.

15. Stubbs, C.W., Springer, M., and Thomas, T.S. (2020). The impacts of testing cadence, mode of instruction, and student density on fall 2020 covid-19 rates on campus. medRxiv.

16. Frazier, P.I., Cashore, J.M., Duan, N., Henderson, S.G., Janmohamed, A., Liu, B., Shmoys, D.B., Wan, J., and Zhang, Y. (2022). Modeling for COVID-19 college reopening decisions: Cornell, a case study. Proc. Natl. Acad. Sci. U. S. A. *119*.

17. Queen, C.S., and Allen, J. (2021). 100 U.S. colleges will require vaccinations to attend in-person classes in the fall. The New York Times.

18. Karthikeyan, S., Nguyen, A., McDonald, D., Zong, Y., Ronquillo, N., Ren, J., Zou, J., Farmer, S., Humphrey, G., Henderson, D., et al. (2021). Rapid, Large-Scale Wastewater Surveillance and Automated Reporting System Enable Early Detection of Nearly 85% of COVID-19 Cases on a University Campus. mSystems *6*, e0079321.

19. Shah, M., Ferra, G., Fitzgerald, S., Barreira, P.J., Sabeti, P.C., and Colubri, A. (2022). Containing the spread of mumps on college campuses. R Soc Open Sci *9*, 210948.

20. Sabeti, P., Botti-Lodovico, Y., Baruch, J., Gutiérrez-Ramos, J.-C., Aguilar, M., Wosen, J., Feuerstein, A., Garde, D., and Herper, M. (2020). A mumps epidemic has a lot to teach colleges about reopening safely in the time of coronavirus. STAT. https://www.statnews.com/2020/10/08/a-mumps-epidemic-has-a-lot-to-teach-colleges-about-reopening-safely-in-the-time-of-coronavirus/.

21. Currie, D.W., Moreno, G.K., Delahoy, M.J., Pray, I.W., Jovaag, A., Braun, K.M., Cole, D., Shechter, T., Fajardo, G.C., Griggs, C., et al. (2021). Interventions to Disrupt Coronavirus Disease Transmission at a University, Wisconsin, USA, August-October 2020. Emerg. Infect. Dis. *27*, 2776–2785.

22. Matrajt, L., and Leung, T. (2020). Evaluating the Effectiveness of Social Distancing Interventions to Delay or Flatten the Epidemic Curve of Coronavirus Disease. Emerg. Infect. Dis. *26*, 1740–1748.

23. Kim, M.-C., Kweon, O.J., Lim, Y.K., Choi, S.-H., Chung, J.-W., and Lee, M.-K. (2021). Impact of social distancing on the spread of common respiratory viruses during the coronavirus disease outbreak. PLoS One *16*, e0252963.

24. Glass, R.J., Glass, L.M., Beyeler, W.E., and Min, H.J. (2006). Targeted Social Distancing Designs for Pandemic Influenza. Emerging Infectious Disease journal *12*, 1671.

25. Tang, S., Xiao, Y., Yuan, L., Cheke, R.A., and Wu, J. (2012). Campus quarantine (Fengxiao) for curbing emergent infectious diseases: lessons from mitigating A/H1N1 in Xi'an, China. J. Theor. Biol. *295*, 47–58.

26. Harris-Lovett, S., Nelson, K.L., Beamer, P., Bischel, H.N., Bivins, A., Bruder, A., Butler, C., Camenisch, T.D., De Long, S.K., Karthikeyan, S., et al. (2021). Wastewater Surveillance for SARS-CoV-2 on College Campuses: Initial Efforts, Lessons Learned, and Research Needs. Int. J. Environ. Res. Public Health *18*.

27. Fielding-Miller, R., Karthikeyan, S., Gaines, T., Garfein, R.S., Salido, R., Cantu, V., Kohn, L., Martin, N.K., Wijaya, C., Flores, M., et al. (2021). Wastewater and surface monitoring to detect COVID-19 in elementary school settings: The Safer at School Early Alert project. medRxiv.

28. Das Swain, V., Xie, J., Madan, M., Sargolzaei, S., Cai, J., De Choudhury, M., Abowd, G.D., Steimle, L.N., and Prakash, B.A. (2021). Empirical networks for localized COVID-19 interventions using WiFi infrastructure at university campuses. bioRxiv.

29. Malloy, M.L., Hartung, L., Wangen, S., and Banerjee, S. (2022). Network-Side Digital Contact Tracing on a Large University Campus. arXiv [cs.NI].

30. Anthes, E. (2021). The Future of Virus Tracking Can Be Found on This College Campus. The New York Times.

31. Specht, I., Sani, K., Botti-Lodovico, Y., Hughes, M., Heumann, K., Bronson, A., Marshall, J., Baron, E., Parrie, E., Glennon, O., et al. (2022). The case for altruism in institutional diagnostic testing. Sci. Rep. *12*, 1857.

32. Student profiles https://www.coloradomesa.edu/institutional-research/student-profiles/index.html.

631 33. Lei, H., Xu, X., Xiao, S., Wu, X., and Shu, Y. (2020). Household transmission of COVID-19-
632 a systematic review and meta-analysis. J. Infect. *81*, 979–997.

633 34. O'Toole, Á., Scher, E., Underwood, A., Jackson, B., Hill, V., McCrone, J.T., Colquhoun, R.,
634 Ruis, C., Abu-Dahab, K., Taylor, B., et al. (2021). Assignment of epidemiological lineages in
635 an emerging pandemic using the pangolin tool. Virus Evol *7*, veab064.

636 35. Outbreak.Info outbreak.info. https://outbreak.info/situation-
637 reports?pango=B.1.429&loc=USA_US-NV&loc=USA_US-CA&selected=USA_US-NV.

638 36. Zhang, J., Litvinova, M., Wang, W., Wang, Y., Deng, X., Chen, X., Li, M., Zheng, W., Yi, L.,
639 Chen, X., et al. (2020). Evolving epidemiology and transmission dynamics of coronavirus
640 disease 2019 outside Hubei province, China: a descriptive and modelling study. Lancet
641 Infect. Dis. *20*, 793–802.

642 37. Meyerowitz, E.A., Richterman, A., Gandhi, R.T., and Sax, P.E. (2021). Transmission of
643 SARS-CoV-2: A Review of Viral, Host, and Environmental Factors. Ann. Intern. Med. *174*,
644 69–79.

645 38. Bi, Q., Wu, Y., Mei, S., Ye, C., Zou, X., Zhang, Z., Liu, X., Wei, L., Truelove, S.A., Zhang,
646 T., et al. (2020). Epidemiology and transmission of COVID-19 in 391 cases and 1286 of
647 their close contacts in Shenzhen, China: a retrospective cohort study. Lancet Infect. Dis.
648 *20*, 911–919.

649 39. Freyja: Depth-weighted De-Mixing (Github).

650 40. Karthikeyan, S., Levy, J.I., De Hoff, P., Humphrey, G., Birmingham, A., Jepsen, K., Farmer,
651 S., Tubb, H.M., Valles, T., Tribelhorn, C.E., et al. (2021). Wastewater sequencing uncovers
652 early, cryptic SARS-CoV-2 variant transmission. medRxiv, 2021.12.21.21268143.

653 41. Grubaugh, N.D., Gangavarapu, K., Quick, J., Matteson, N.L., De Jesus, J.G., Main, B.J.,
654 Tan, A.L., Paul, L.M., Brackney, D.E., Grewal, S., et al. (2019). An amplicon-based
655 sequencing framework for accurately measuring intrahost virus diversity using PrimalSeq
656 and iVar. Genome Biol. *20*, 8.

657 42. Deng, X., Garcia-Knight, M.A., Khalid, M.M., Servellita, V., Wang, C., Morris, M.K.,
658 Sotomayor-González, A., Glasner, D.R., Reyes, K.R., Gliwa, A.S., et al. (2021).
659 Transmission, infectivity, and neutralization of a spike L452R SARS-CoV-2 variant. Cell
660 *184*, 3426–3437.e8.

661 43. Hodcroft, E.B., Domman, D.B., Snyder, D.J., Oguntuyo, K.Y., Van Diest, M., Densmore,
662 K.H., Schwalm, K.C., Femling, J., Carroll, J.L., Scott, R.S., et al. (2021). Emergence in late
663 2020 of multiple lineages of SARS-CoV-2 Spike protein variants affecting amino acid
664 position 677. medRxiv.

665 44. Wohl, S., Giles, J.R., and Lessler, J. (2021). Sample size calculation for phylogenetic case
666 linkage. PLoS Comput. Biol. *17*, e1009182.

667 45. Office of the Commissioner FDA takes key action in fight against COVID-19 by issuing
668 emergency use authorization for first COVID-19 vaccine. U.S. Food and Drug
669 Administration. https://www.fda.gov/news-events/press-announcements/fda-takes-key-
670 action-fight-against-covid-19-issuing-emergency-use-authorization-first-covid-19.

671 46. Center for Devices, and Radiological Health At-Home OTC COVID-19 Diagnostic Tests.
672 U.S. Food and Drug Administration. https://www.fda.gov/medical-devices/coronavirus-
673 covid-19-and-medical-devices/home-otc-covid-19-diagnostic-tests.

674 47. Wilm, A., Aw, P.P.K., Bertrand, D., Yeo, G.H.T., Ong, S.H., Wong, C.H., Khor, C.C., Petric,
675 R., Hibberd, M.L., and Nagarajan, N. (2012). LoFreq: a sequence-quality aware, ultra-
676 sensitive variant caller for uncovering cell-population heterogeneity from high-throughput
677 sequencing datasets. Nucleic Acids Res. *40*, 11189–11201.

678 48. viral-pipelines (Github).

679 49. Campbell, F., Cori, A., Ferguson, N., and Jombart, T. (2019). Bayesian inference of
680 transmission chains using timing of symptoms, pathogen genomes and contact data. PLoS
681 Comput. Biol. *15*, e1006930.

682

683

Figure 1

Figure 1. The *Lookout* system implements real-time monitoring of COVID-19 cases, including spatial, longitudinal, and social patterns of disease burden

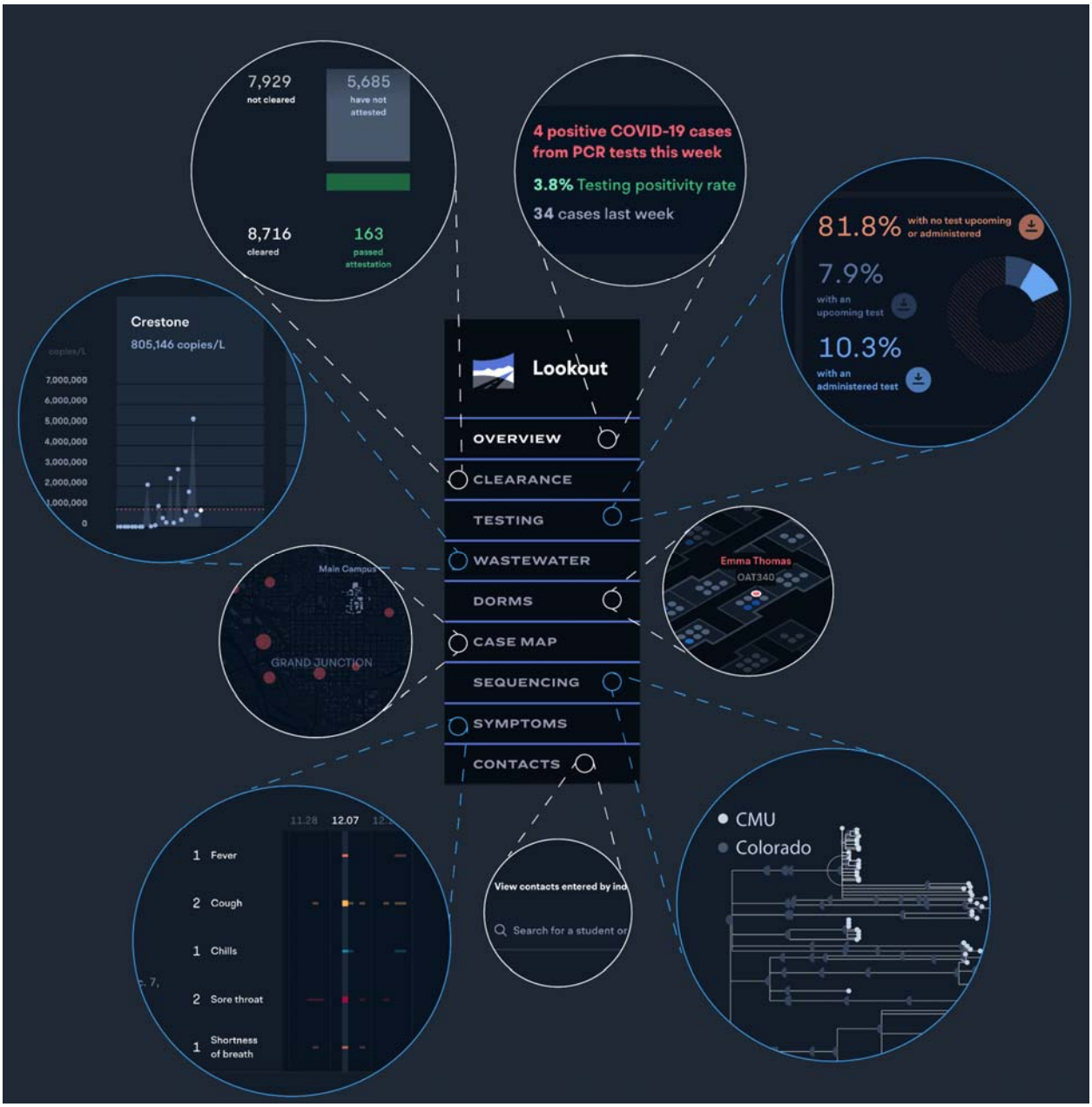

The *Lookout* tool integrated clinical diagnostic test results, student metadata, viral genome sequences from diagnostic specimens, and wastewater viral titers. A demo with representative synthetic data is available at https://sentinel.network/lookout-demo-campus/. **Overview**. Current data on community case burden, test volume, high-incidence groups, and symptom and exposure attestation. **Clearance**. Full-population counts of the individuals complying with the training and symptom attestation requirements for campus entry. **Testing**. Reports of positive tests in the past 7 days as well as the volume of tests scheduled, taken, and missed for the

current week. **Testing - Baseline**. A view of “back to campus” testing measures tracking the number of tests administered over time against the amount needed to successfully test the entire population before a return to campus. **Wastewater**. Viral load over time, measured on a per-sewershed basis, aligned with individual test results from the same residence halls. **Dorms**. Views showing spatial position of residence hall cases on a per-floor basis. Individuals may be selected to view their associated membership groups (*i.e.*, potential close contacts), present attestation, test, and isolation status. Main view page depicts campus-wide case density. **Case Map**. Large-area view of case locations for members of the university community who live off-campus, with hot spots for locations of high case density. **Sequencing**. Phylogenetic tree showing the ancestry and clustering of viral genomes collected from university cases. Individual cases may be selected to view other individuals who are members of the same cluster, as well as specific attributes of the individual. Viral lineages are noted. **Symptoms**. Timelines depict reported symptoms for students or staff, including fever, cough, chills, sore throat, shortness of breath, loss of smell/taste, and runny nose. **Contacts**. Rapid search for the list of contacts reported by cases, and their associated contact information. **Lookup**. Review of information in *Lookout* for a given individual, including group affiliations, test result history, symptom history, attestation history, and contact history.

Figure 2

Figure 2. Data types, incidence rates, and epidemiological risk factors for SARS-CoV-2 positivity on Colorado Mesa University’s campus

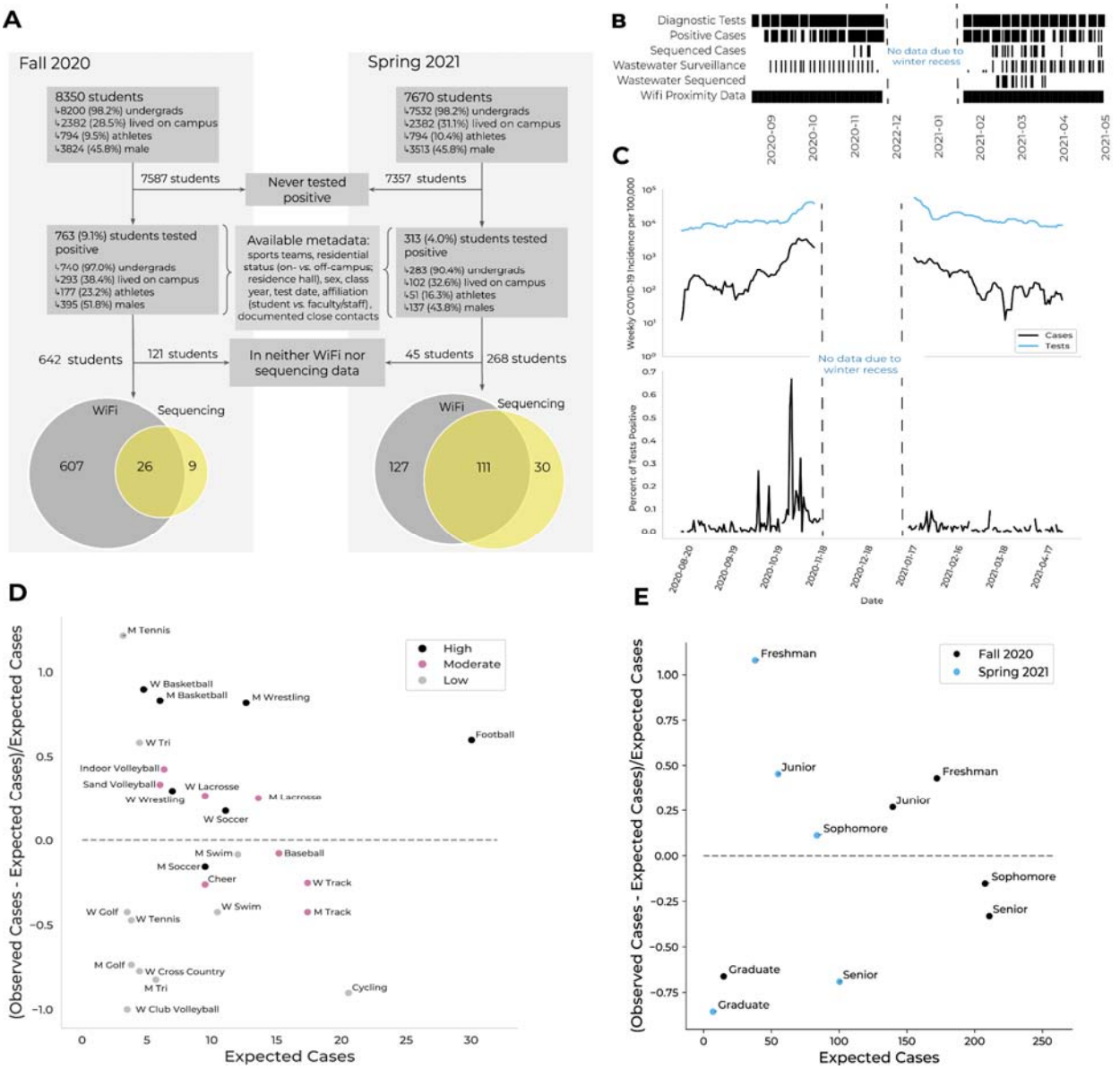

A. Cohort description. A subset of students at Colorado Mesa University (CMU) tested positive for COVID-19 *via* reflexive or random surveillance RT-qPCR testing. CMU provided demographic and behavioral metadata for each case. The majority of students who tested positive were enrolled in the wifi proximity program (gray). A subset of positive samples were available for viral genomic sequencing (yellow). **B.** Timeline showing data collection timepoints (black) by data type during the Fall and Spring semesters. Data not shown for November 21–January 18 due to winter recess. **C.** Upper: Weekly COVID-19 incidence (black) and number of tests conducted (blue) over the 2020–2021 academic year. Lower: Percent positivity rate. Data not shown for November 21–January 18 due to winter recess. **D.** The difference between the number of cases observed and the number of cases expected (based on sports team player count and scaled by the number of cases expected; *y* axis) *vs.* the number of cases expected (*x* axis), per sports team. The dashed line at y=0 separates teams with more (above) or fewer (below) cases observed than expected. Teams are colored by contact level (legend). M refers to men's teams and W to women's teams. **E.** The difference between the number of cases

observed and the number of cases expected (based on class size and scaled by the number of cases expected; *y* axis) *vs.* the number of cases expected (*x* axis), per class year. The dashed line at *y* = 0 separates classes with more (above) or fewer (below) cases observed than expected. Classes are colored by semester (legend).

Figure 3

Figure 3. Social connectivity network from the wifi co-location data identifies behavioral trends that correlate with case counts

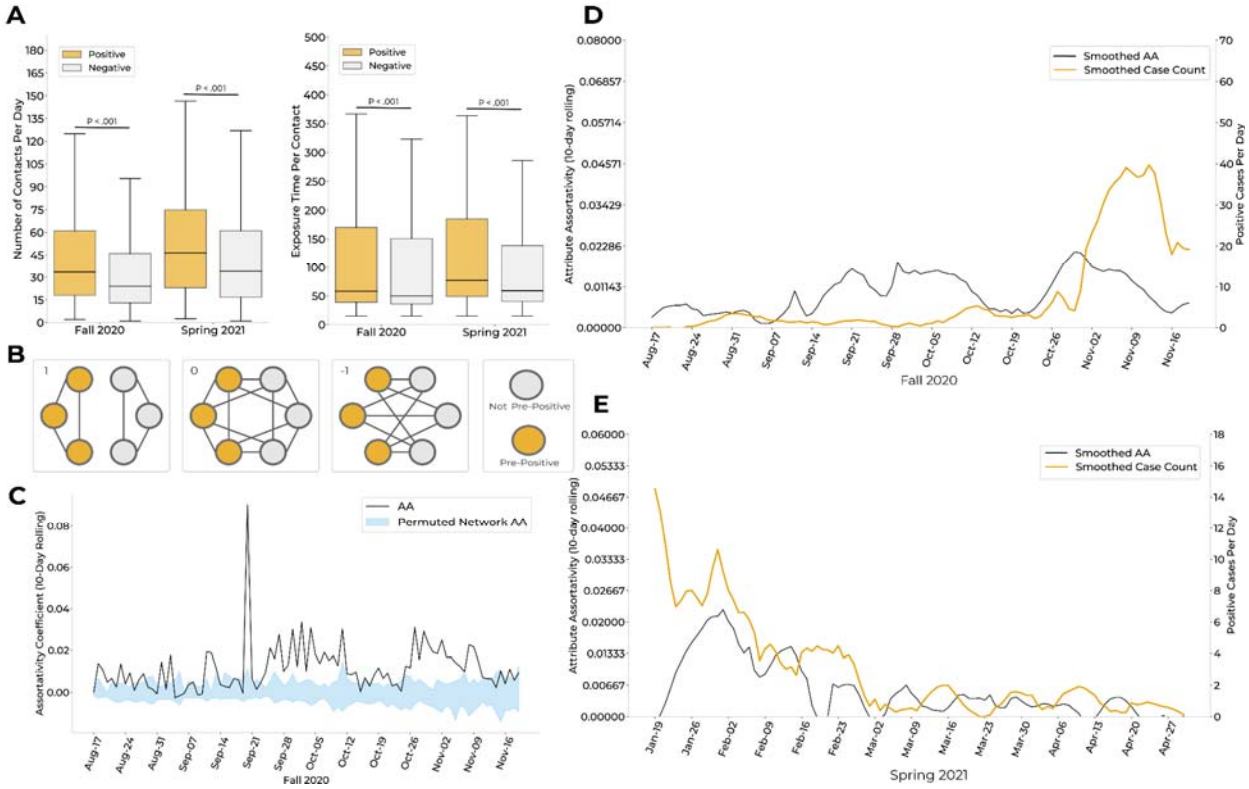

A. Left: Distributions of daily contacts (Appendix Table 11) for students who tested positive over the course of each semester (orange) *vs.* those who remained negative (gray) over the course of each semester. Effect sizes, 9.5 (Fall; positive median = 33.5, negative median = 24), 12.5 (Spring; positive median = 46.5, negative median = 34). Right: Distributions of average exposure time per contact (Appendix Table 11), in minutes, for cases (orange) *vs.* those who remained negative (gray). Effect sizes, 8.2 (Fall; positive median = 58, negative median = 49.8), 11.8 (Spring; positive median = 77, negative median = 58.8). **B**. Visual representation of the network metric attribute assortativity (AA; described in Supplemental Methods). We depict network scenarios where the AA coefficient is equal to 1, 0, or -1. When AA = 1, pre-positive individuals, defined as those within 10 days prior to their positive test, have interactions only with pre-positive individuals, and vice versa. When AA = 0: pre-positives individuals have an equal likelihood of interactions with pre-positive individuals and non-pre-positive individuals. When AA = -1, pre-positive individuals have interactions only with non-pre-positive individuals, and vice versa. Positive AA values indicate a higher propensity for within-group interactions, while negative values indicate a higher propensity for between-group interactions. **C**.

Comparison of per-semester AA for individuals within a 10 day window of a positive test (*i.e.*, pre-positives) *vs.* those who never tested positive (*i.e.*, negatives). 95% confidence intervals (CI; blue) were calculated by permuting pre-positive and negative labels for individuals within the proximity network each day, 40 times. The AA of the proximity network (black) was above the upper bound of the CI for 69.4% (66/95 days) of the Fall 2020 semester, implying significance at $p < 0.025$. Only Fall 2020 is presented here; methodology and results were consistent for Spring 2021 (Appendix Figure 8). **D-E**. Comparison of smoothed case counts and smoothed AA for Fall 2020 (**D**) and Spring 2021 (**E**). Smoothing *via* the Savitzky-Golay filter (window length = 17, polynomial order = 4).

Figure 4

Figure 4. Case clusters and lineages identified by viral genomic sequencing, and comparison of genomic cases to reported social network degree distributions

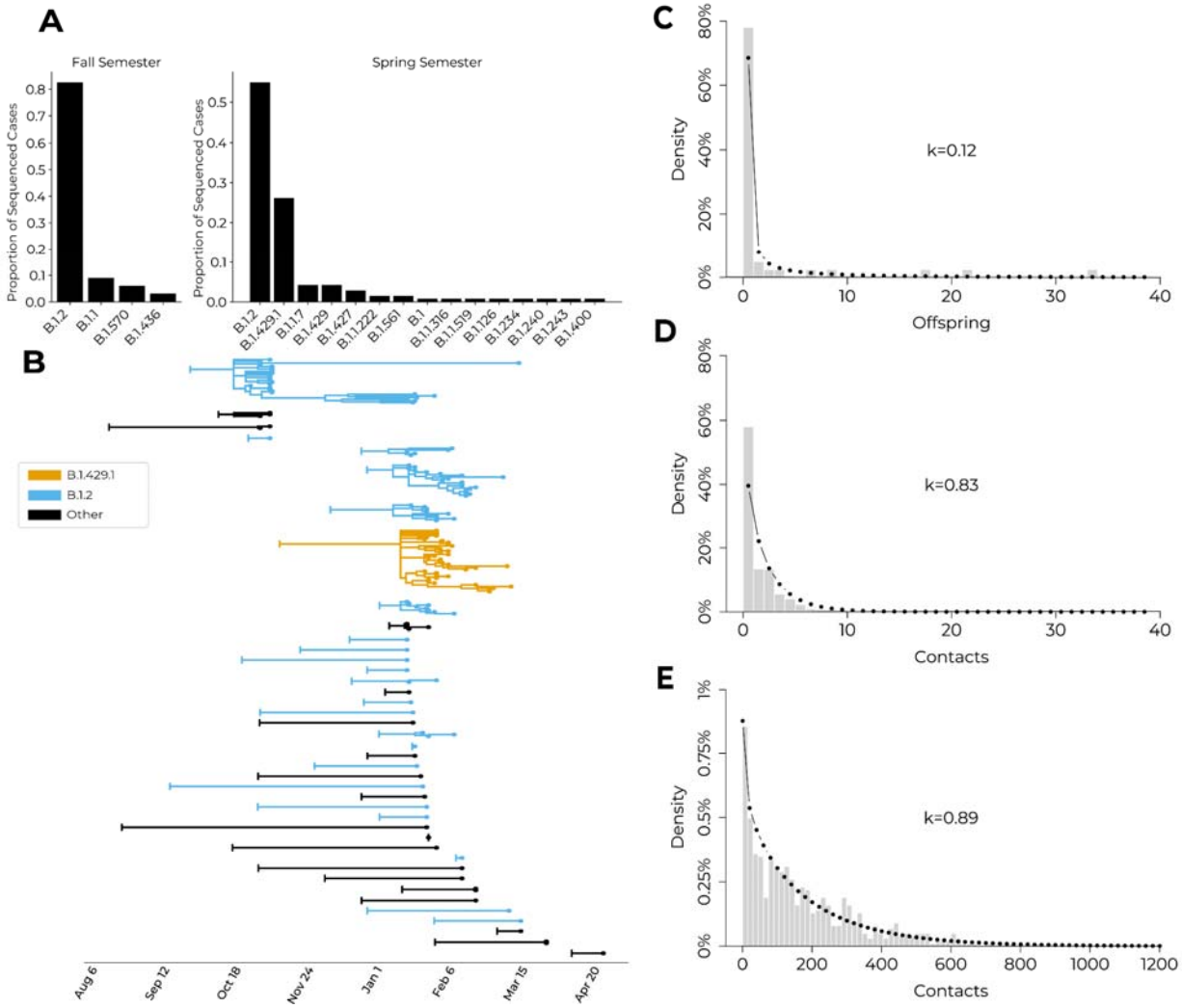

A. Pango lineage proportions for university cases during the Fall 2020 and Spring 2021 semesters. **B.** Phylogenetic trees for inferred introductions to the campus community with branch lengths scaled to time. B.1.2 clusters (blue), the B.1.429.1 cluster (orange), and all other lineages (black). Vertical bar on the left of each introduction indicates the inferred ancestral root

date of each university case or case cluster; cases are tip dots at right of each tree. **C.** Distribution of offspring from phylogenetic clusters, with a negative binomial distribution fit and overlaid (dotted line) to quantify overdispersion. Unique introductions and resulting offspring were grouped into phylogenetic clusters; mean=2.56 offspring/introduction; k=0.13 (dispersion parameter). **D.** Distribution of the number of contacts from positive individuals identified during contact tracing, with a negative binomial distribution fit and overlaid (dotted line). Contacts were defined as any individuals with interaction dutations greater than 15 minutes in the 48-hour period prior to positive test or symptom onset; mean=1.71 contacts per positive individual; k=0.83. **E.** Distribution of the number of wifi contacts observed from positive individuals, with a negative binomial distribution fit and overlaid (dotted line). Contacts were defined as individuals with interaction durations greater than 15 minutes in the 48-hour period prior to testing positive or symptom onset; mean=177.94 contacts per positive individual; k=0.89.

Figure 5

Figure 5. Wastewater surveillance and sequencing for measurement of aggregate viral load, identification of circulating lineages, and comparison with viral genomes from contemporaneous clinical cases

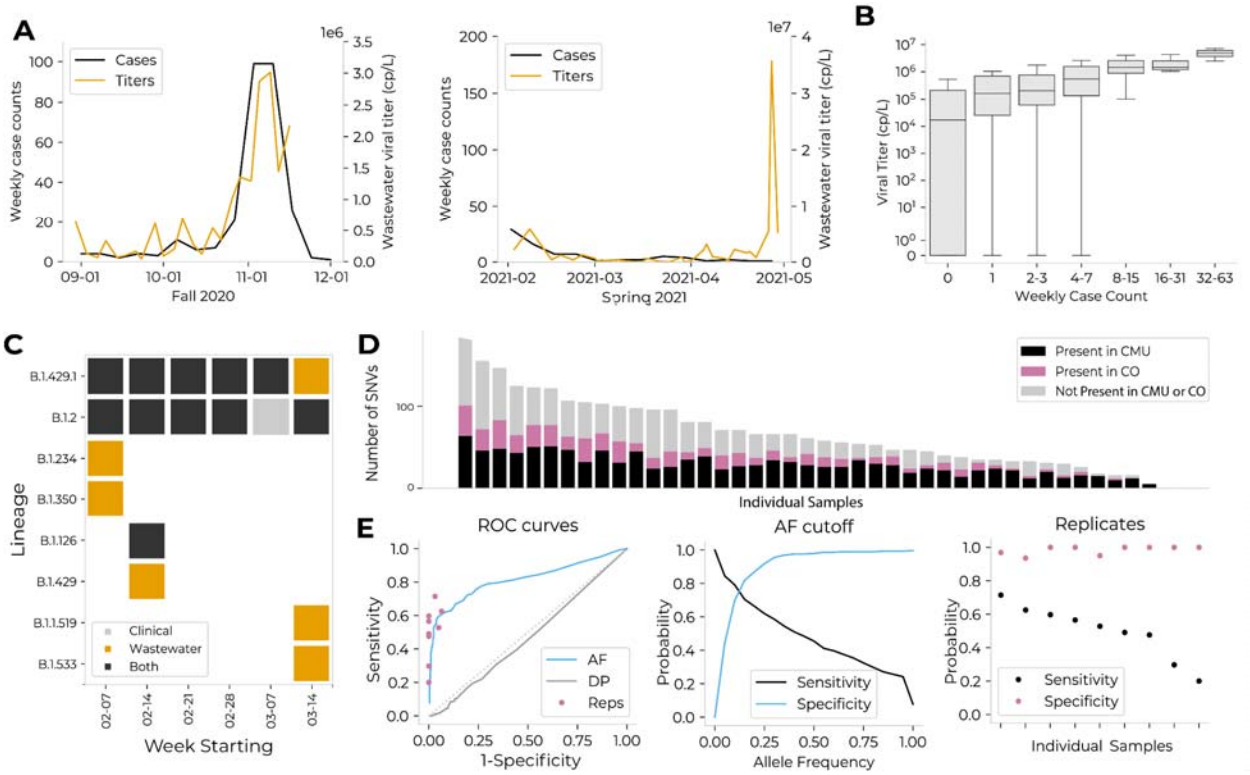

A. Average wastewater viral titers (orange) *vs.* weekly residential case count (black). Residential case counts were calculated relative to the subsets of dorms monitored (75% of residential population in Fall 2020; 99% in Spring 2021). There was an anomalous peak in wastewater viral titer observed in April, which could be due to technical error, differential shedding patterns, or undiscovered positive individuals. **B.** Viral titer (*y* axis) *vs.* binned weekly

case count (*x* axis; binned by powers of 2) for each wastewater sample. Viral titer and case count were significantly associated *via* Fisher's exact test (p=0.04) and Spearman's correlation=0.40 (p<0.001). **C.** Lineages detected on campus via wastewater or clinical sequencing. **D.** The number of single nucleotide variants (SNVs) detected in wastewater samples; each bar represents a single sample. Individual samples are organized on the *x* axis in order of total number of SNVs. For each sample, SNVs are categorized by whether they were present in clinical sequences from CMU (black), in clinical sequences from Colorado (pink), or in neither (gray). On average, 51% of SNVs in a single wastewater sample were not found in CMU clinical samples, and 36% were not found in Colorado clinical samples. **E.** Comparison of quality control methods to remove SNVs not validated by presence in Colorado clinical sequences. The three methods compared are: 1) allele frequency (AF), or discarding SNVs present at an allele frequency below a given threshold; 2) read depth (DP), or discarding SNVs located at a site with a read depth below a given threshold; and 3) replicates (Reps), or discarding SNVs not present within both of two technical replicates of a given sample. These analyses are limited to the nine samples for which technical replicates exist. Left: ROC curves for each of the three filters. Middle: Sensitivity and specificity for allele frequency-based quality control method. Right: Sensitivity and specificity for replicate-based quality control method.

Figure 6

Figure 6. A multimodal exploration of the novel lineage B.1.429.1 *via* clinical and environmental genomic sequencing, wifi proximity analyses, transmission reconstruction networks, and experimental validation

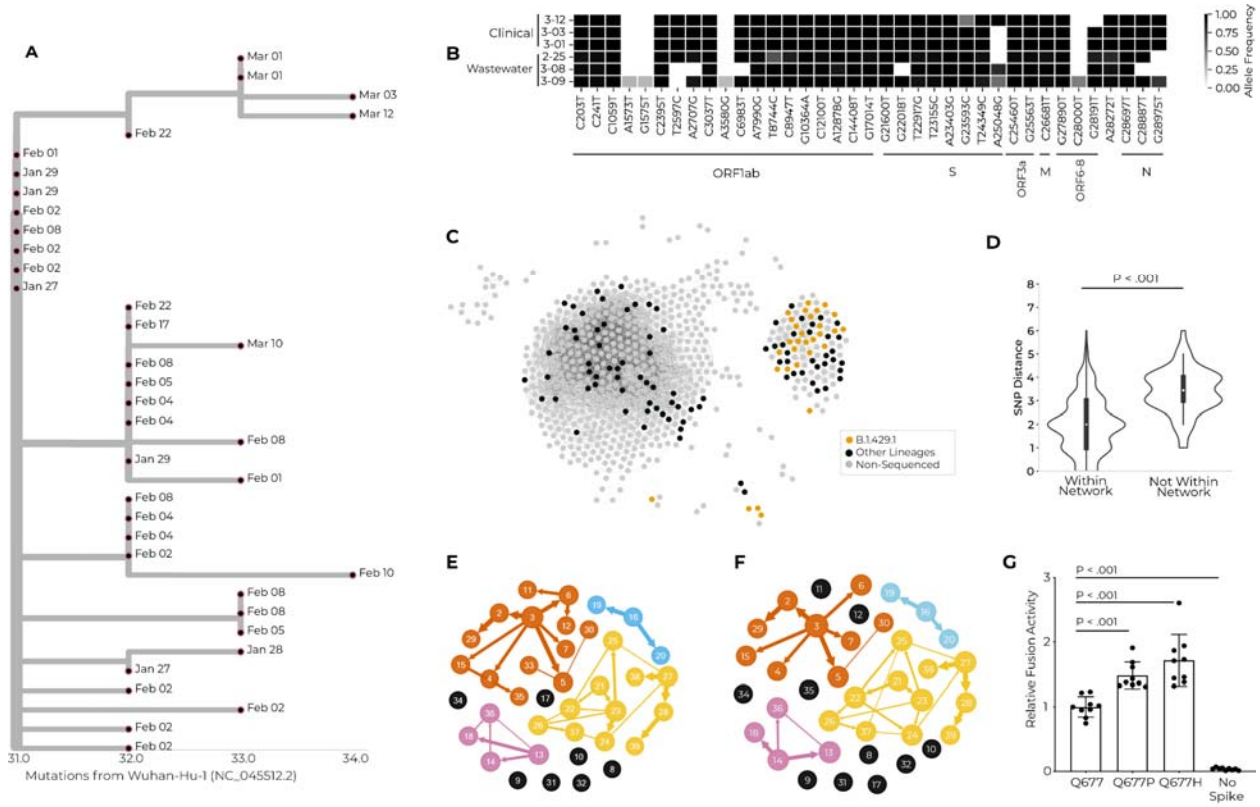

A. Phylogenetic tree showing the relationship between cases within the B.1.429.1 case cluster. Tree tips are anchored at their dates of sample collection, and branch lengths are scaled by maximum likelihood. One-to-many polytomies depict clonal amplification, with multiple cases with the same ancestral node rather than as a series of bifurcating branches. **B.** Three wastewater samples and three clinical samples (*y* axis), all of the B.1.429.1 lineage. The three wastewater samples had B.1.429.1 as the sole identified lineage, and were extracted from Site 3, for which residential halls B and M are the only upstream contributors. Shown in comparison are clinical viral genomes from three students believed to have contributed effluent to these wastewater samples, based on residential status and test date. The *x* axis represents all single-nucleotide variants present in at least one wastewater sample with 25% allele frequency or greater. SNVs are grouped by genomic position. **C.** Social proximity network for interactions occurring between two individuals who are both within a 10-day window prior to testing positive. Edges in this network represent one or more simultaneous wifi access point connections. Each node represents a positive individual. The node color represents their sequencing status (legend). **D.** Comparison of genetic distance for individuals of the B.1.429.1 lineage who are or are not connected *via* the social proximity network shown in (**C**). Effect size = 1 mutation. **E-F.** Transmission reconstruction network for B.1.429.1 cases created with genomic information as well as manual contact tracing data (**E**) or wifi-inferred 10-day contact data (**F**). **G.** Results of cell-cell fusion activity of viral pseudotypes with the ancestral allele, or with the S:Q677P or S:Q677H amino acid changes, relative to a luminescent control with no Spike protein expressed.

Figure 7

Figure 7: A step-wise approach to outbreak surveillance with consideration for resource limitations

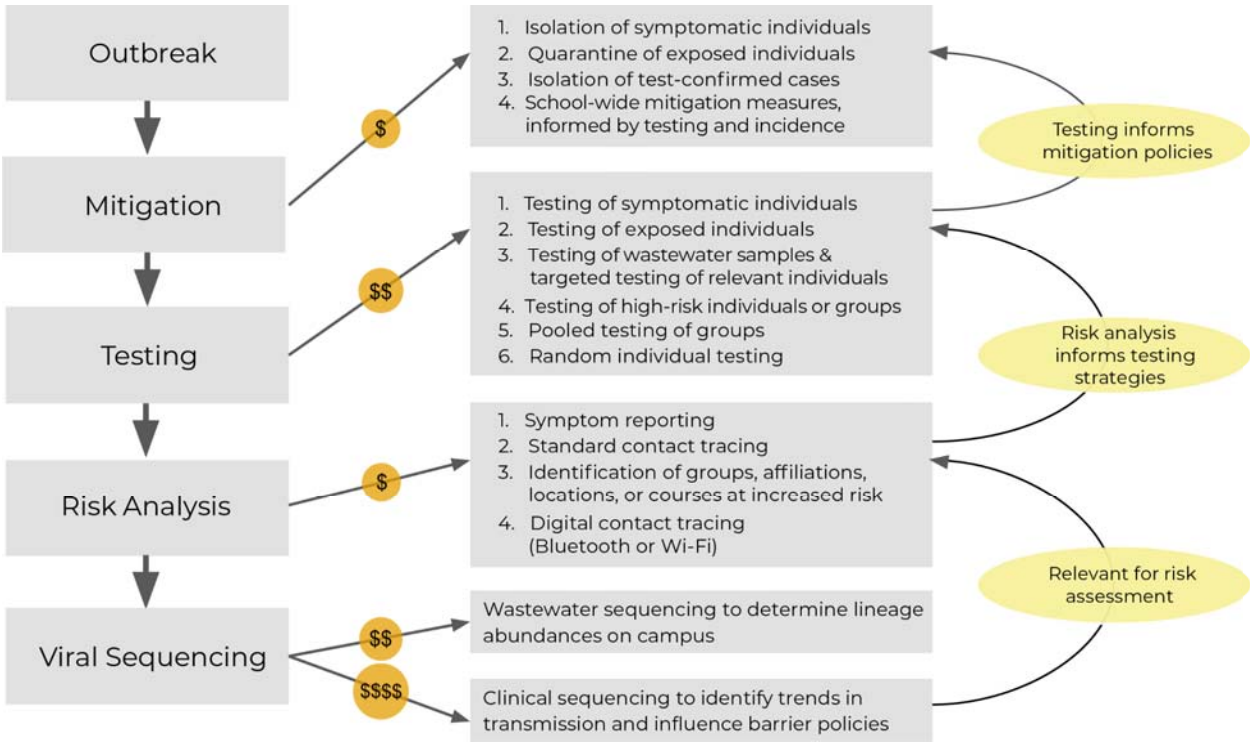

Illustration of the flow of actions to employ during an institutional outbreak, with delineation of relative cost and information feedback cycles. During an outbreak, initial mitigation measures can be deployed prior to and independent of a surveillance program. A basic surveillance program will first incorporate testing, the results of which will inform additional mitigation policies. Next, analyses of case attributes can be used to assess the risk of infection for specific sub-populations; these analyses will allow for development of specialized, directed testing strategies Finally, while more expensive, viral genomic sequencing of clinical or environmental samples can be used to identify transmission trends and to detect emergent viral genomic variation with potential public health or clinical relevance. This in turn can be used to inform institutional policy and the intensity of mitigation efforts. Actions involving solely personnel time are the least expensive to implement (*i.e.*, mitigation, risk analyses), while actions requiring both personnel and laboratory consumables are more expensive (*i.e.*, testing), and actions requiring laboratory consumables, highly trained personnel, and prolonged instrument time are most expensive to implement (*i.e.*, viral sequencing).

Appendix Figure 1

Appendix Figure 1. Incidence rates at Colorado Mesa University (CMU), with surrounding areas for context, and epidemiological risk factors for SARS-CoV-2 positivity at CMU

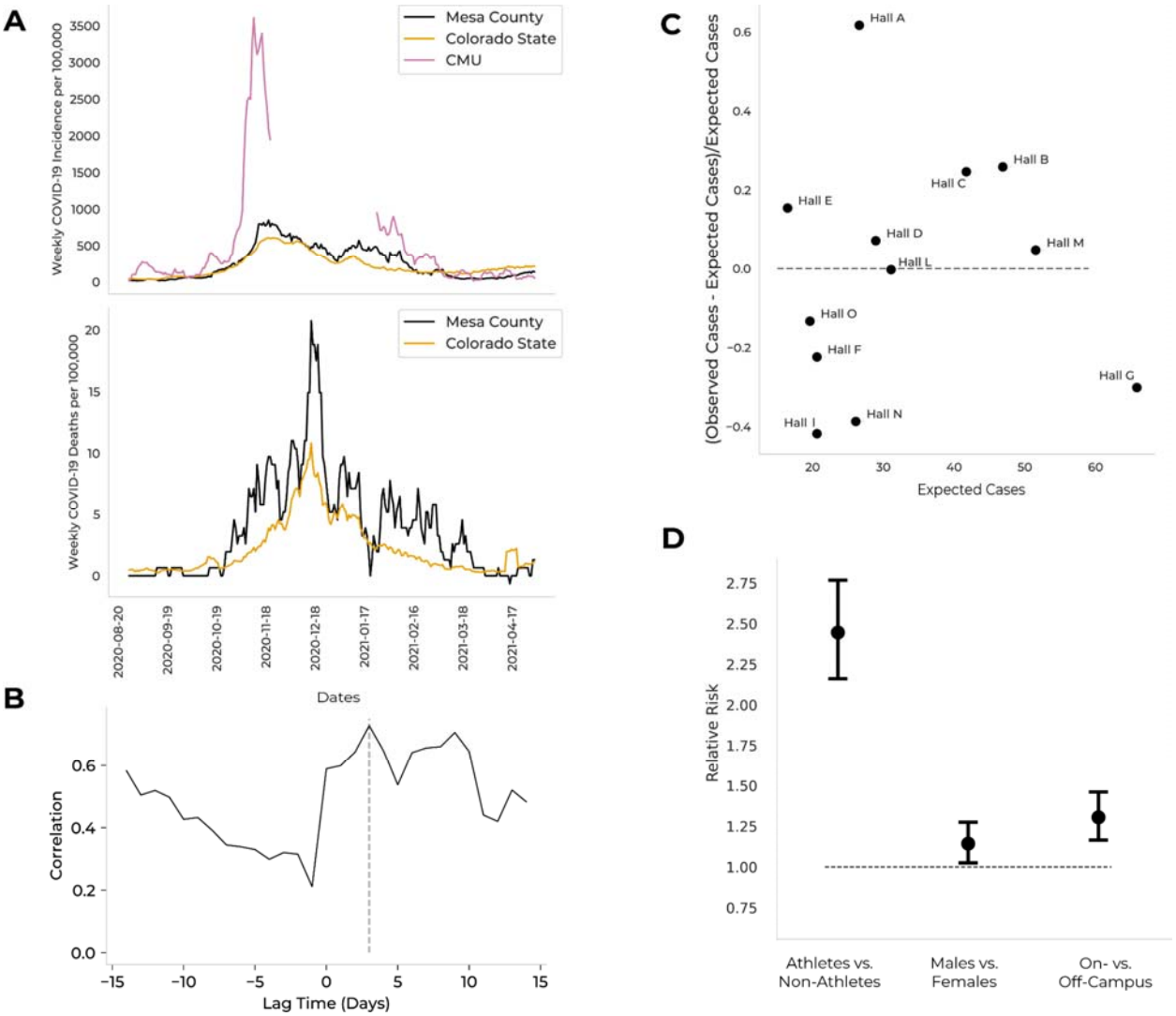

A. Weekly COVID-19 incidence at Colorado Mesa University (CMU; pink), in Mesa County (black), and in Colorado (orange) over the 2020–2021 academic year (upper). Weekly COVID-19 death rate in Mesa County (black) and in Colorado (orange) over the 2020–2021 academic year (lower). Data from CMU were not analyzed from November 21–January 18 due to winter recess. The correlations between CMU incidence rates and Mesa County incidence rates (correlation = 0.73, lag = 3 days) and Mesa County death rates (correlation = 0.48, lag = 8 days) were tested with lag times between -14 days (0 days for deaths) and 14 days, and the maximum correlations and corresponding lag times are reported. **B.** The correlation between CMU incidence rates and Mesa County incidence rates *vs.* the lag time. The dashed line at $y = 3$ indicates the lag time that maximizes the cross-correlation. **C.** The difference between the number of cases observed and the number of cases expected (given residence hall population size and scaled by number of cases expected) *vs.* the number of cases expected, per residence hall. The dashed line at $y = 0$ separates halls with more (above) or fewer (below) cases observed than expected. **D.** Relative risk (RR) of testing positive for COVID-19 given sports team membership (athletes *vs.* non-athletes), sex (males *vs.* females), or residential status (on- *vs.* off-campus). Circles represent the relative risk, with whiskers extending to the upper and

lower bounds of the 95% confidence interval. The dashed line at RR = 1 represents the null hypothesis (*i.e.*, that there is no association between the risk factor and test positivity). An RR greater than 1 implies that the first group listed (*i.e.*, athletes, males, or on-campus students) had a greater risk of testing positive than the second group listed (*i.e.*, non-athletes, females, or off-campus students).

Appendix Figure 2

Appendix Figure 2. Detection of outbreak groups using viral genomic sequencing of cases

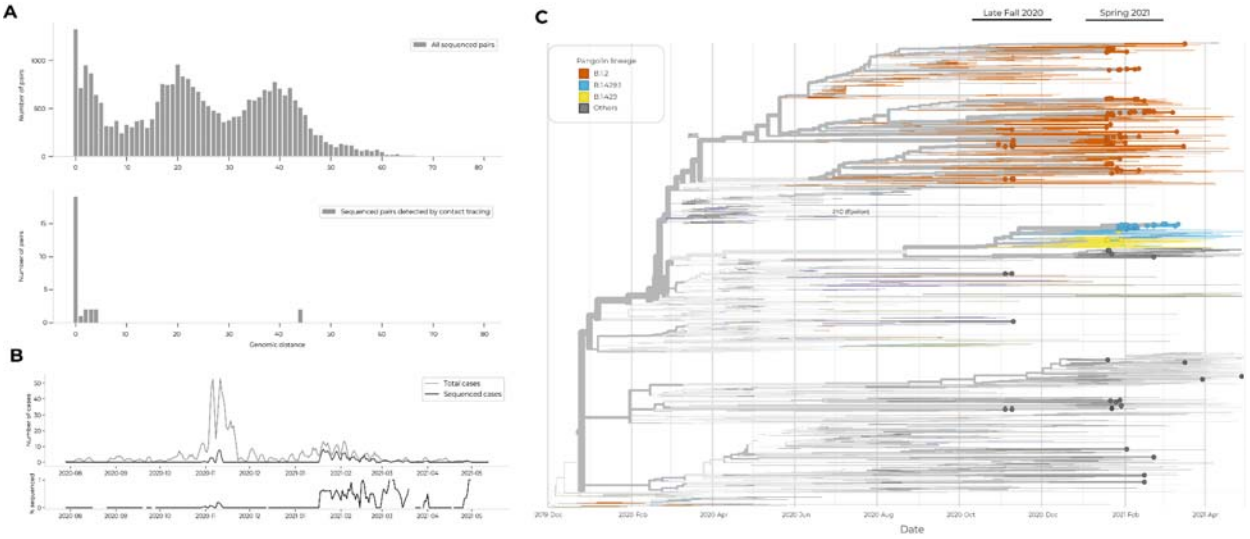

A. Distributions of genetic distance for all pairs of viral genomes (upper) and for pairs of viral genomes from positive individuals sharing interactions reported during contact tracing (lower). We sequenced viral samples from 18 pairs of positive individuals where one of the individuals identified the other as a close contact, and 11 pairs where both individuals identified one another as a close contact. Two outlier pairs had a genetic distance of 44 SNVs. In each of these pairs, an individual testing positive at the end of January 2021 had virus of the B.1.2 lineage and indicated close contact with an individual who tested positive in early February (5-6 days later) with virus of the B.1.429.1 lineage. **B.** Sequencing of positive cases via genomic surveillance across both semesters. Sequencing began October 2020, capturing cases associated with a Halloween-related outbreak. Shown are the total number of cases (top, thin line), total number of sequenced cases (top, bolded line), and percent of positive cases that were sequenced (bottom). **C.** Phylogenetic placement and temporal sampling of viral genomes sequenced from CMU clinical diagnostic tests. CMU nodes are depicted as dots among a global tree of contextual sequences, weighted toward sequences collected from Colorado and surrounding states, but including uniformly-sampled genomes from all dates and geographic regions, as well as genomes close in genetic distance to CMU sequences. Interactive version available at https://auspice.broadinstitute.org.

Appendix Figure 3

Appendix Figure 3. Summary of wastewater surveillance implemented at Colorado Mesa University across Fall 2020 and Spring 2021

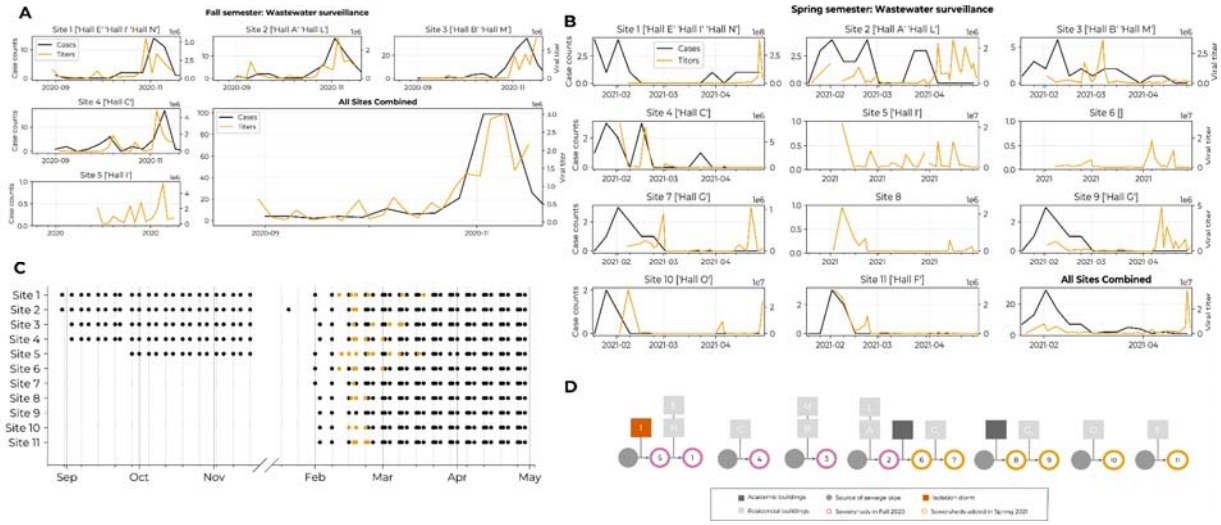

A-B. Comparison of wastewater viral titer (orange) and weekly case count (black) for each wastewater site in the Fall semester (**A**) and Spring semester (**B**). **C.** Sample collection frequency for wastewater surveillance in the 2020–2021 academic year. Wastewater samples were collected twice weekly in the Fall across 5 sites, and three times weekly in the Spring across 11 sites. Each dot represents an independent collection event, with dots shown in orange representing sequenced wastewater samples. **D.** Schematic showing which residential or academic buildings (squares) contributed effluent to each monitored wastewater site (circles). Residence hall I (red square) housed a small number of students who had tested positive and were in isolation. Wastewater sites are represented by circles, with filled-in gray circles representing sites utilized to collect baseline measurements where there were no upstream contributors to that particular sewage system. Sites shown in pink were added in Fall 2020 and remained in use into Spring 2021, while sites shown in orange were added in Spring 2021.

Appendix Figure 4

Appendix Figure 4. Predictions of COVID-19 incidence rates in Colorado Mesa University residence halls *via* a linear regression model

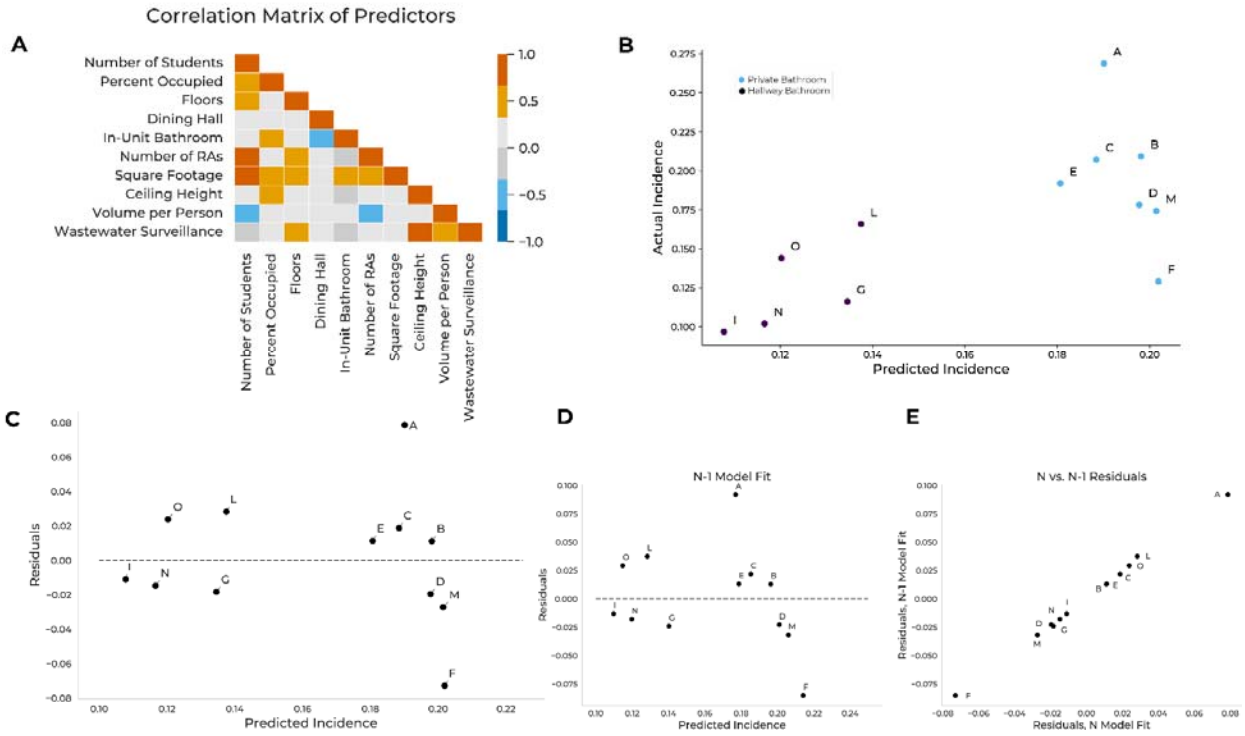

A. Descriptive attributes of residence halls, including number of students, percent occupied (number of available beds / number of students), number of floors, the presence of a meal plan requirement ('dining hall'), the presence of an in-unit bathroom ('private bath'), the number of resident advisors (RAs), square footage, ceiling height, volume per person, and the presence of wastewater surveillance, were used as predictors in the regression model. Non-zero correlation coefficients between pairs of predictive variables indicate multicollinearity. **B.** Observed incidence rates *vs.* predicted incidence rates, by residence hall. Predictions come from the model that minimized the Akaike and Bayesian Information Criteria. Colors indicate the difference in predicted incidence associated with a private *vs.* a hallway bathroom. **C.** Residuals *vs.* predicted incidence rates, by residence hall. Root-mean-square-error = 3.6%. **D.** Residuals *vs.* predicted incidence rates, from leave-one-out cross-validation, by residence hall. Leave-one-out cross-validation (*i.e.*, *N*-1 model fit, where *N* = number of residence halls) was conducted such that each hall's incidence rate was predicted *via* a linear model whose coefficients were determined with training data from all other halls. Root-mean-square-error = 4.2%. **E.** Residuals from the leave-one-out cross-validation (*N*-1 model fit) *vs.* residuals from the full model (*N* model fit).

Appendix Figure 5

Appendix Figure 5. On-campus presence, as inferred by wifi proximity data, by semester and by user category

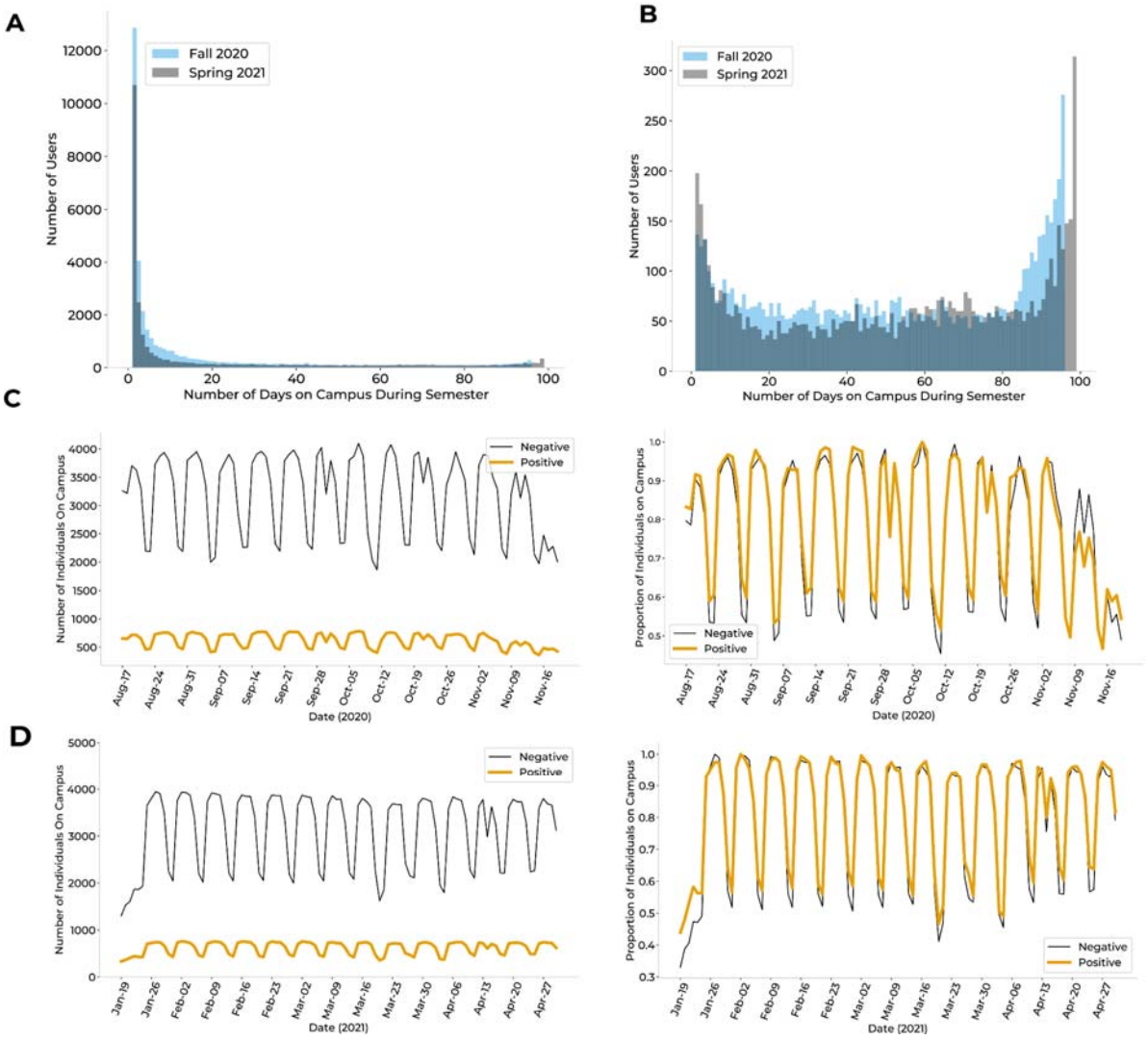

A. Distribution of the number of days present on campus for all users found in the wifi network, colored by semester. **B.** Distribution of the number of days present on campus for all users found in the wifi network after removal of unauthenticated users, non-students, and infrequent users, colored by semester. This cleaned wifi proximity network was used for all future analyses. **C.** Number (left) and proportion (right) of positive students (orange) and negative students (black) on campus by day for Fall 2020 (Appendix Table 11). There was no significant difference in the proportion distributions ($p = 0.282$). We found a significant correlation in the trends of the proportion distributions (Pearson Correlation: .976, $p < .0001$). **D.** Number (left) and proportion (right) of positive students (orange) and negative students (black) on campus by day for Spring 2021 (Appendix Table 11). There was no significant difference in the proportion distributions ($p = 0.248$). We found a significant correlation in the trends of the proportion distributions (Pearson Correlation: .99, $p < .0001$).

Appendix Figure 6

Appendix Figure 6. Wifi network access patterns by building and by semester.

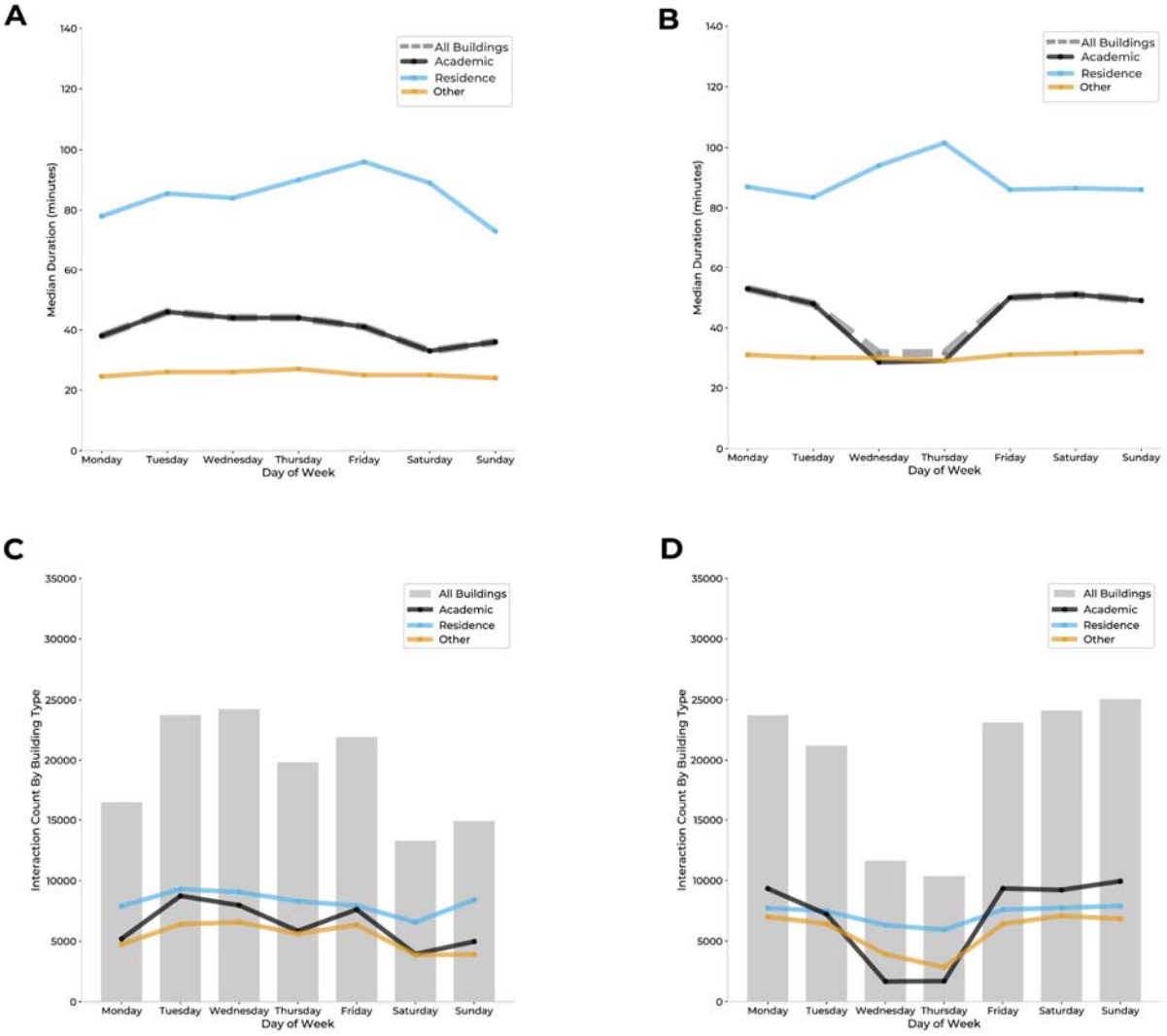

A-B. Median duration of access point connections in minutes, per day of the week and by building type (academic, residential, other, or all buildings) for Fall 2020 (**A**) and Spring 2021 (**B**; Appendix Table 11). **C-D.** Daily number of AP connections, per day of the week and by building type (academic, residential, other, or all buildings) for Fall 2020 (**C**) and Spring 2021 (**D**; Appendix Table 11).

Appendix Figure 7

Appendix Figure 7. Interaction patterns of individuals and of pairs of individuals by testing status

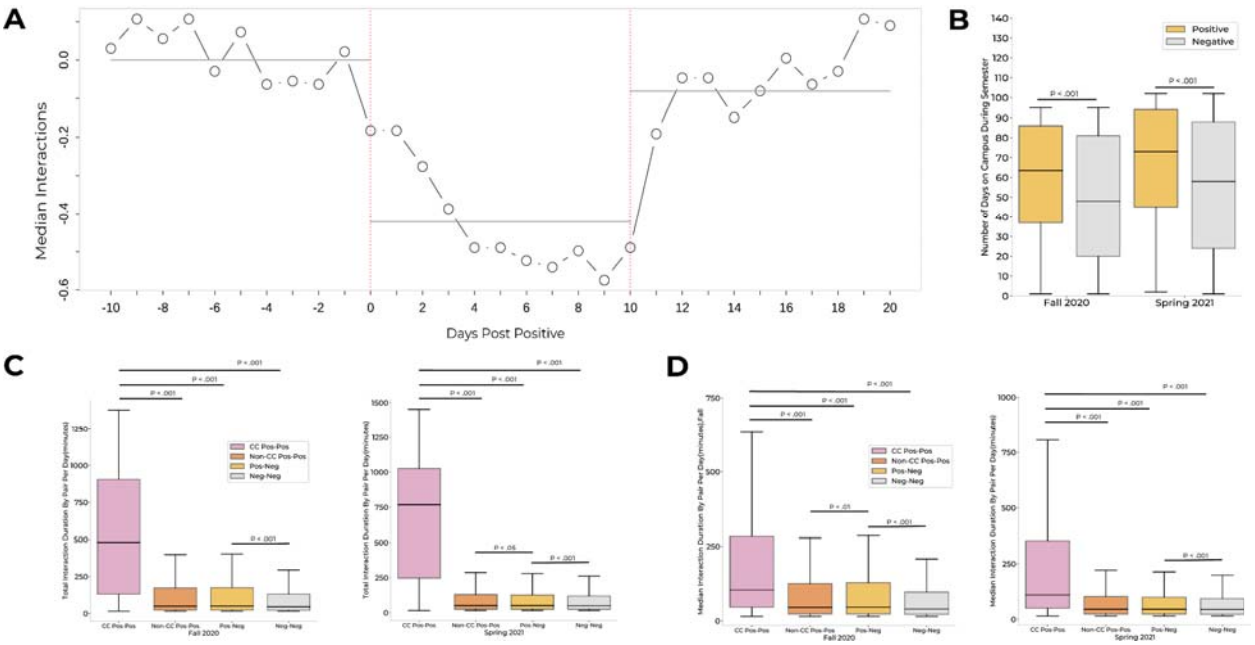

A. Median number of wifi contacts per day for the 30-day period surrounding the isolation period of positive cases. Day 0 was calculated as the earliest of symptom onset date and test date. Black lines indicate the median number of contacts (y-axis) per individual for every day across the period (x-axis). **B.** The number of days on campus for positive (orange) *vs.* negative (gray) individuals. Effect sizes, 15 days (median positive: 66; median negative: 51; Fall 2020) and 16 days (median positive: 76; median negative: 60; Spring 2021). Gray bars indicate averages for three 10-day periods: pre-isolation, isolation, and post-isolation. **C.** Distributions of total pairwise daily interaction duration , for pairings categorized by testing status: CC Pos-Pos, pairs of pre-positive individuals with an association reported in manual contact tracing; Non-CC Pos-Pos, pairs of pre-positive individuals without an association reported in manual contact tracing; Pos-Neg, pairs of one pre-positive and one negative individual; Neg-Neg, pairs of two negative individuals. Pre-positive individuals were defined as students within the 10-day window prior to testing positive. **D.** Distributions of median interaction duration by pair per day, for pairings categorized by test status (see above description). Positive individuals were defined as students within the 10-day window prior to testing positive. See Appendix Table 11 for equations used in panels **A**, **C**, and **D**.

Appendix Figure 8

Appendix Figure 8. Comparison of randomness vs true assortativity within the wifi proximity network in conjunction with semester daily case counts

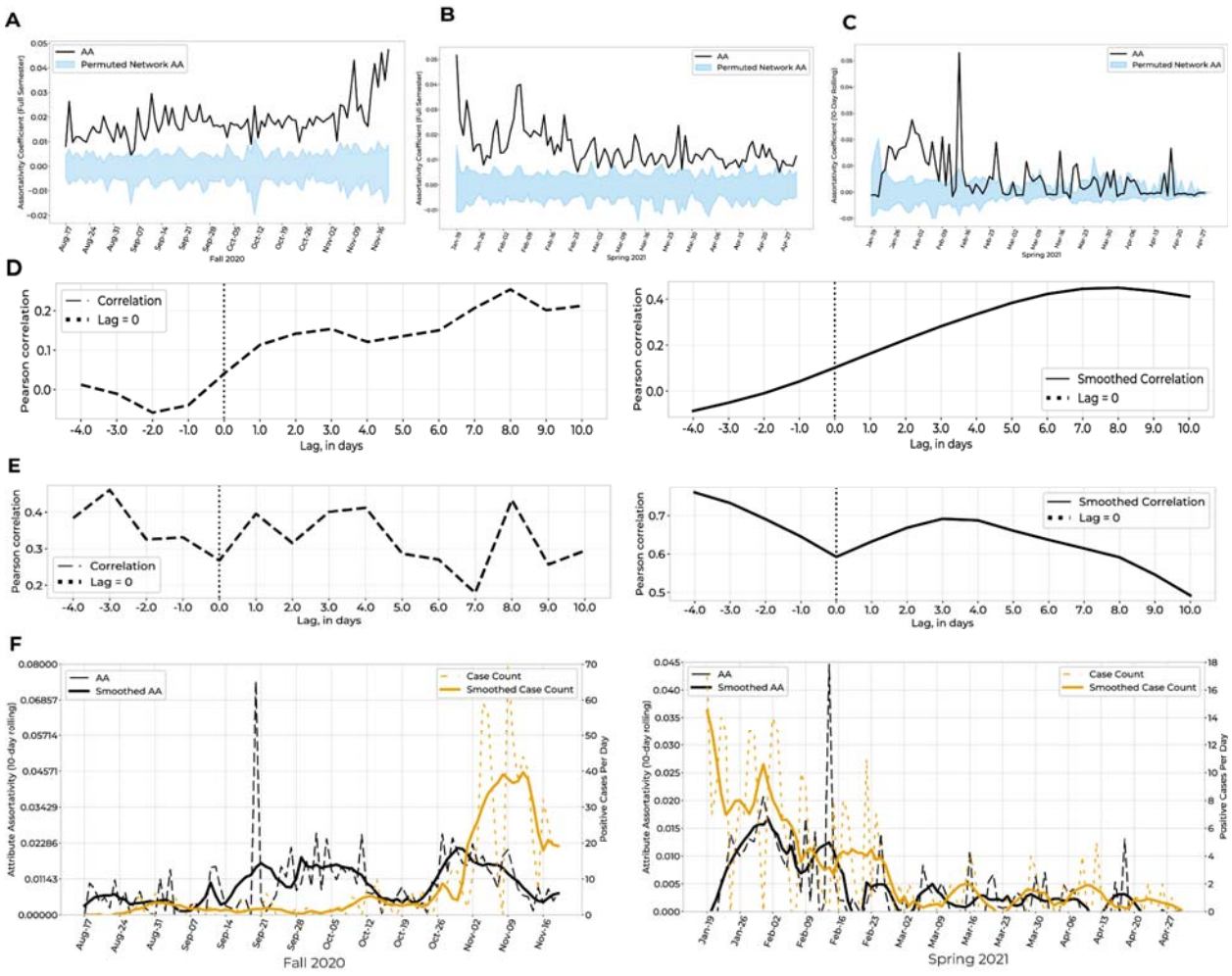

A-B. Comparison of attribute assortativity (AA) for positives *vs*. negatives, for Fall 2020 (**A**) and Spring 2021 (**B**). 95% Confidence Intervals (CI; blue) were calculated by permuting positive and negative labels for individuals within the proximity network each day. The AA of the proximity network (black) was above the upper bound of the CI for 98.9% (94/95 days) in the Fall 2020 semester and 98%(100/102 days) in the Spring 2021 semester, indicating significance with $p < 0.025$. **C.** We calculated the same metric with altered groupings: pre-positives (all individuals within a 10-day window prior to their positive test) *vs.* negatives (individuals not within a 10-day window prior to a positive test, regardless of overall semester testing status). The AA of the proximity network (black) was above the upper bound of the CI for 37.2% (38/102 days) in the Spring 2021 semester, indicating significance with $p < 0.025$. **D.** Correlations between daily AA (pre-positives *vs*. negatives) and daily case count with varying lag times, where both AA and case count are non-smoothed (top) or smoothed using Savitzky Golay filter (bottom), for Fall 2020. The highest correlation occurs with a lag time such that AA preceded the case count by 8 days (Pearson correlation = 0.253 for non-smoothed, 0.449 for smoothed). **E.** Cross-correlations between daily AA (pre-positives *vs*. negatives) and daily case count with varying lag times, where both AA and case count are non-smoothed (top) or smoothed using Savitzky Golay filter (bottom), for Spring 2021. The highest correlation occurs with lag time such that AA preceded the case count by 4 days (Pearson correlation=0.411 for non-smoothed; 3 days for

smoothed, with correlation = 0.691). **F.** Unsmoothed case counts and unsmoothed AA *vs.* smoothed case counts and smoothed AA for Fall 2020 (left) and Spring 2021 (right).

Appendix Figure 9

Appendix Figure 9. Comparison of assortativity within the wifi proximity network when defining the "pre-positive" attribute as positive individuals without pairwise associations within the contact tracing data.

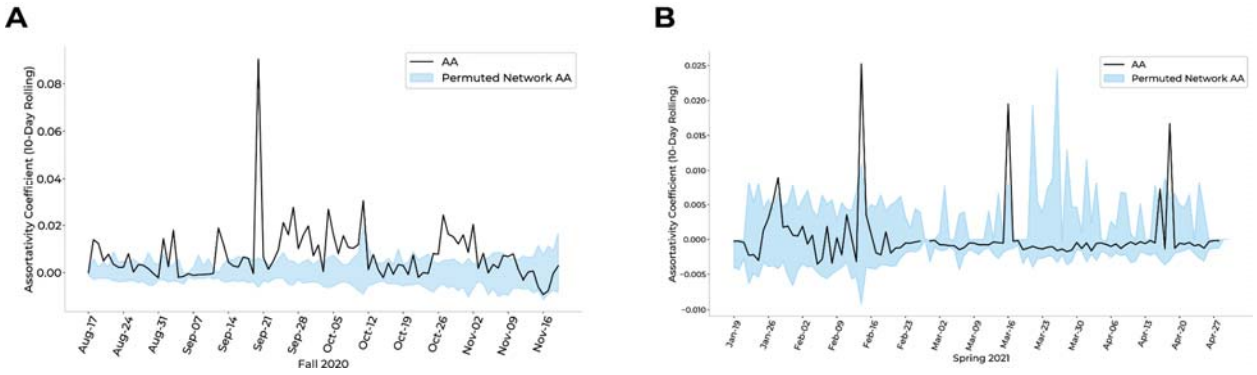

A-B. Comparison of attribute assortativity (AA) for pre-positives *vs*. negatives, for Fall 2020 (**A**) and Spring 2021 (**B**). 95% Confidence Intervals (CI; blue) were calculated by permuting pre-positive and negative labels for individuals within the proximity network each day. We calculated the same metric with pre-positives defined as individuals within a 10-day window prior to their positive test without pairwise associations with other pre-positive individuals in the contact tracing data and negatives defined as individuals not within a 10-day window prior to a positive test, regardless of overall semester testing status. The AA of the proximity network (black) was above the upper bound of the CI for 45.2% (43/95 days) of the Fall 2020 semester (**A**) and 8.8% (9/102 days) of the Spring 2021 semester (**B**), indicating significance with $p < 0.025$.

Appendix Figure 10

Appendix Figure 10. Sequenced wastewater samples, though subject to increased degradation, are of similar genome coverage as sequenced clinical samples

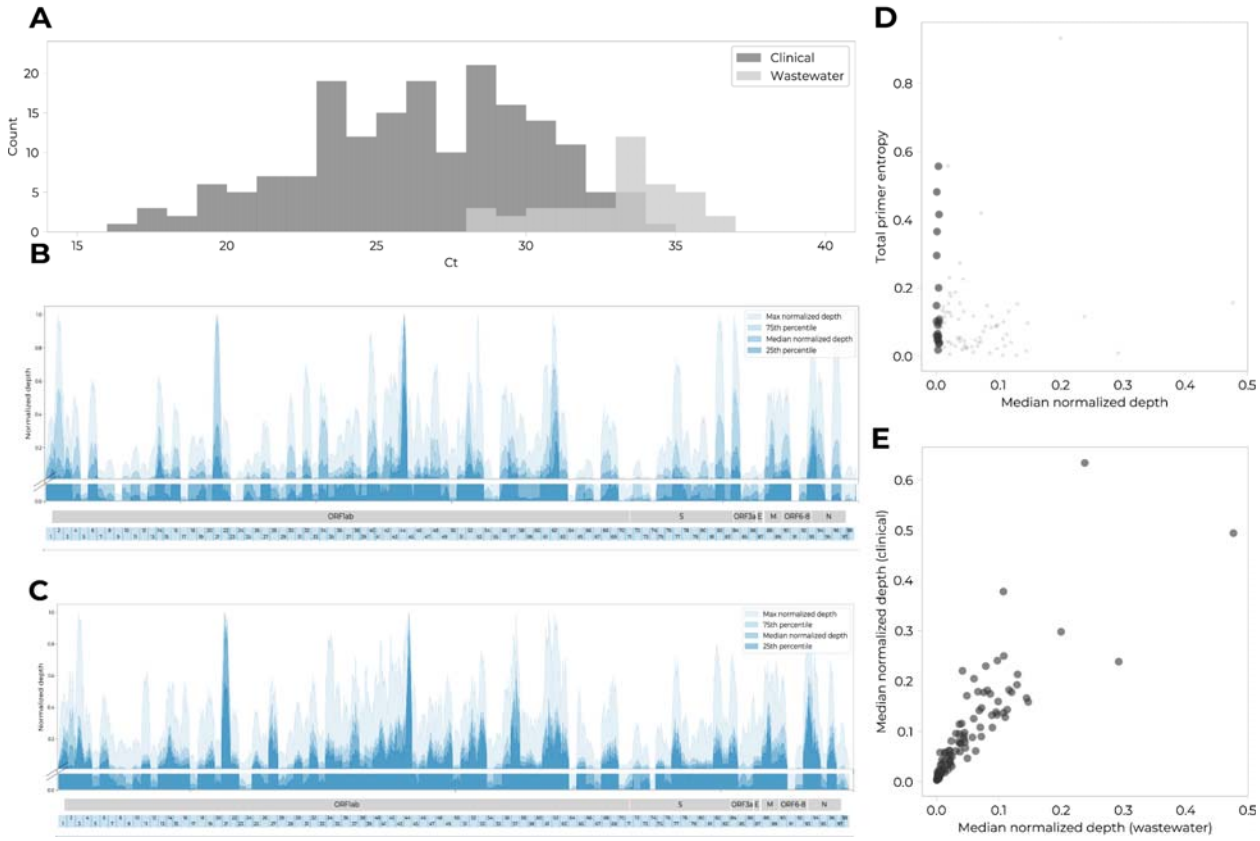

A. Cycle thresholds (Ct) for sequenced wastewater and clinical samples from Colorado Mesa University. **B-C.** Median normalized read depth per base, across all wastewater (**B**) and clinical (**C**) samples. The coloring indicates quartiles across all wastewater or clinical samples. Regions of lower depth in wastewater sequencing are of similarly low depth in clinical sequencing. **D.** Comparison of average amplicon read depth (*x* axis) and average amplicon primer entropy (*y* axis) for wastewater samples. We found no correlation between amplicon read depth and primer entropy (Pearson correlation coefficient of r = .02, p = 0.81). The 20 amplicons with lowest median normalized depth are shown as larger circles. **E.** Comparison of median normalized depth per amplicon between wastewater (*x* axis) and clinical (*y* axis) samples. There is a linear correlation between corresponding amplicons (Pearson correlation coefficient of r = 0.86; p<0.001).

Appendix Figure 11

Appendix Figure 11. Presence of previously undetected mutations in sequenced wastewater samples suggests sequencing error

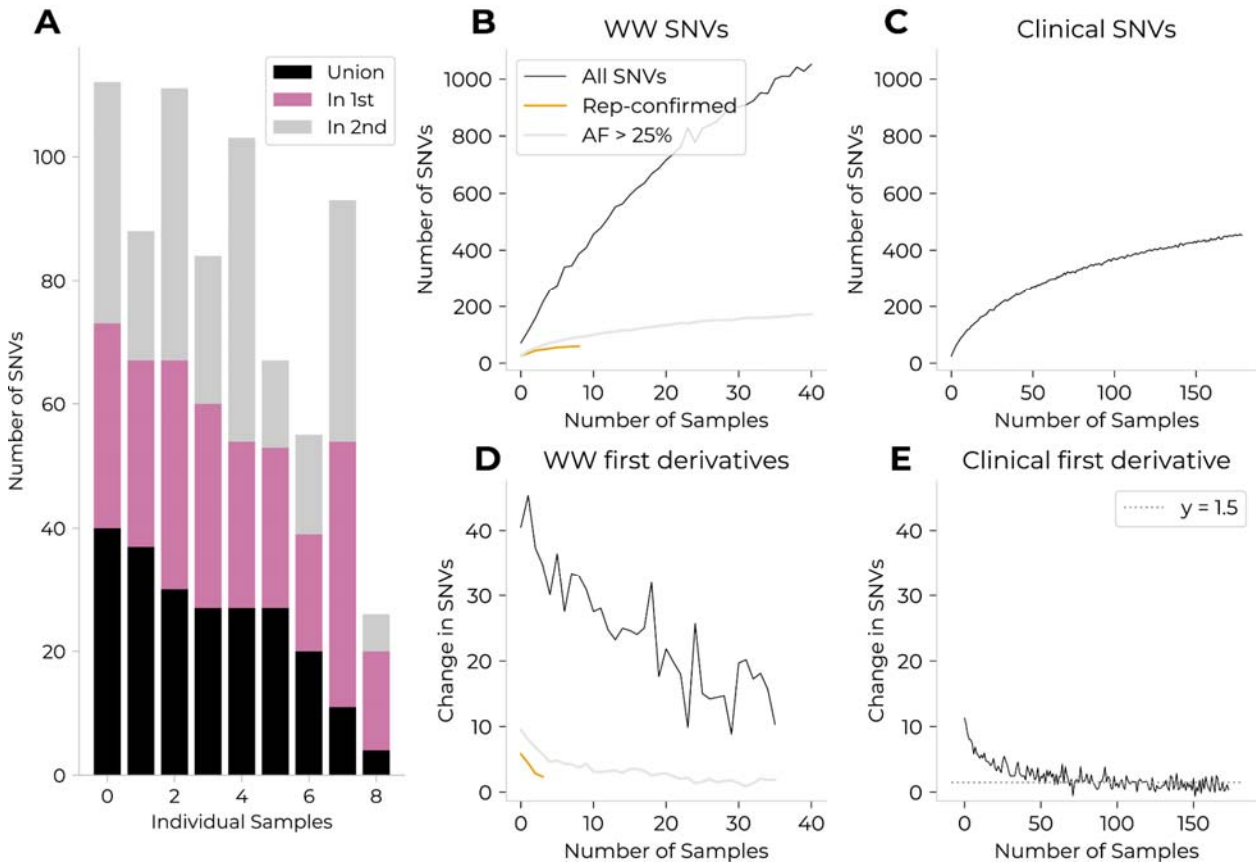

A. Distribution of single-nucleotide variants (SNVs) that were present in only one technical duplicate (pink and gray) or in both duplicates (black). The samples are ordered relative to the number of replicate-confirmed SNVs. **B.** Predictions for the number of unique SNVs that can be expected for a given number of wastewater samples, calculated per the methodology described in the Supplemental Methods. We additionally calculated the number of unique SNVs that would be expected to pass an allele frequency quality control threshold of 25% (gray) or to be seen in at least both technical replicates of any given sample (orange). **C**. Predictions for the number of unique consensus-level SNVs that can be expected for a given number of clinical samples, calculated per the methodology described in the Supplemental Methods. **D.** Smoothed (window=5) first derivative of unique wastewater SNVs per sample. Legend is the same as in panel (**B**). This highlights that while the first derivatives for both replicate-confirmed SNVs (orange) and SNVs with an allele frequency greater than 25% (gray) approaches a rate of 1-3 new SNVs per sample, the first derivative for all SNVs of any allele frequency (black) approaches a rate of >10 new SNVs per sample. **E.** Smoothed (window=5) first derivative of unique clinical consensus-level SNVs per sample. This highlights that the first derivative for all consensus-level SNVs seen in clinical samples approaches a rate of 1.5 new SNVs per sample. The comparison between (**D**) and (**E**) lends support to the hypothesis that most SNVs seen in wastewater samples are spurious, and that either confirming SNVs via technical replicates or a high allele frequency threshold is sufficient to remove most spurious SNVs.

Appendix Figure 12

Appendix Figure 12. Social proximity patterns, transmission reconstruction networks, and experimental viral phenotypes associated with B.1.429.1

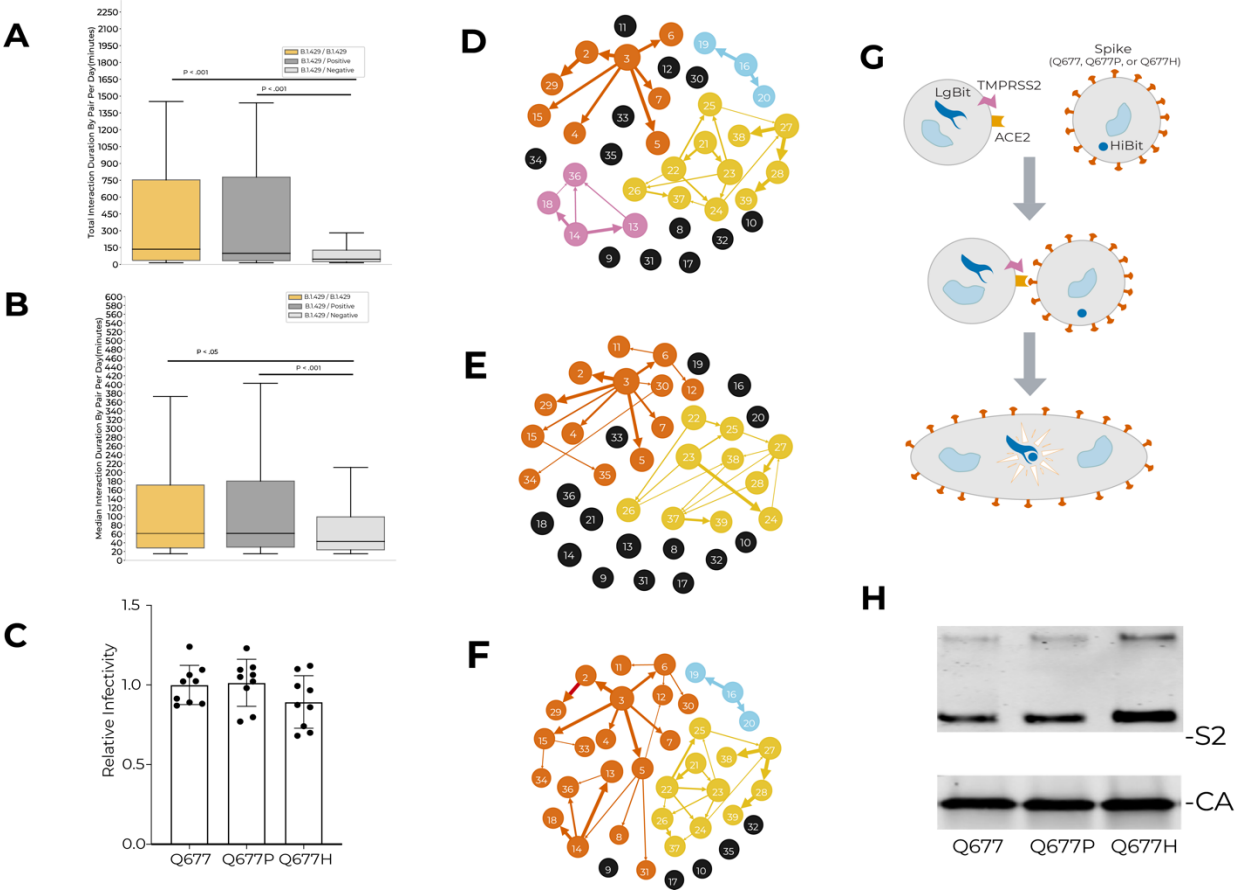

A. Distributions of total daily interaction duration (Appendix Table 11), per pair and per day, for pairs of B.1.429.1-positive (within 10 days of positive tests), non-B.1.429.1-positive (within 10 days of positive tests), and negative individuals. Non-B.1.429.1-positive individuals are defined as positive individuals whose viral genome was not sequenced or was sequenced and determined not to be B.1.429.1. **B.** Distributions of median daily interaction duration (Appendix Table 11), per pair per day, for pairs of B.1.429.1-positive (within 10 days of positive tests), non-B.1.429.1-positive (within 10 days of positive tests), and negative individuals. **C.** Results of infectivity of viral pseudotypes with the ancestral allele, or with the S:Q677P or S:Q677H amino acid changes, relative to a luminescent control with no Spike protein expressed. **D-F.** Transmission reconstruction network for B.429.1 cases created with solely genomic information (**D**), solely manual contact tracing data (**E**), and both genomic information and wifi-inferred 2-day contact data (**F**). **G.** Conceptual diagram showing the experimental strategy for assessing the fusogenicity of the S:Q677H or S:Q677P amino acid changes relative to the ancestral residue, using two populations of cells: one expressing the modified Spike protein on the cell surface, and a second expressing the ACE2/TMPRSS2 receptors. The two populations were combined and fusion signal was assessed via HiBit-LgBit luminescent reporter. **H.** Western blot illustrating successful creation of viral pseudotype particles bearing Spike protein with S:677Q, S:Q677H, and S:Q677P.

Appendix Table 1

Appendix Table 1. Properties of residence halls at Colorado Mesa University

Hall	Number of Students	Percent Occupancy	Number of Floors	Dining Hall Requirement	In-unit Bathroom	Number of RAs	Square Footage	Ceiling Height	Volume per Person	Number of COVID-19 Cases
Hall A	160	0.89	3	1	1	5	46695	8	2334.75	43
Hall B	282	0.94	4	1	1	4	96429	8	2735.57	59
Hall C	251	0.88	4	1	1	8	80100	8	2552.99	52
Hall D	174	0.94	4	0	1	6	59360	8	2729.12	31
Hall E	99	0.83	3	0	1	4	28080	8	2269.09	19
Hall F	124	0.97	4	1	1	5	45996	9.67	3586.95	16
Hall G	396	0.91	4.25	1	0	15	93650	9.67	2286.86	46
Hall I	124	0.73	3	1	0	4	42507	8	2742.39	12
Hall L	187	0.93	3	1	0	6	42883	8	1834.57	31
Hall M	310	0.97	5	1	1	10	72500	8	1870.97	54
Hall N	157	0.79	3	1	0	6	44178	8	2251.11	16
Hall O	118	0.81	5	1	0	5	43843	8	2972.41	17

Structural and communal properties of residence halls. Volume per person was calculated as square footage * ceiling height / number of students per hall and serves as a proxy for air volume per person. Hall G has 4 floors and a partial basement, covering approximately 25% of the square footage of the other floors.

Appendix Table 2

Appendix Table 2. Properties of athletic teams at Colorado Mesa University

Team	Number of Students	Contact Level	Season	Location	Number of COVID-19 Cases
Women's Golf	11	Low	both	outdoor	<5
Women's Club Volleyball	11	Low	both	indoor	<5
Men's Golf	12	Low	both	outdoor	<5
Women's Tennis	12	Low	both	outdoor	<5
Women's Cross Country	14	Low	fall	outdoor	<5
Men's Triathlon	18	Low	both	outdoor	<5
Cycling	65	Low	both	outdoor	<5
Women's Swimming	33	Low	both	indoor	6

Men's Tennis	10	Low	both	outdoor	7
Women's Triathlon	14	Low	both	outdoor	7
Cheerleading	30	Moderate	both	indoor	7
Men's Soccer	30	High	fall	outdoor	8
Sand Volleyball	19	Moderate	spring	outdoor	8
Women's Basketball	15	High	both	indoor	9
Women's Wrestling	22	High	both	indoor	9
Indoor Volleyball	20	Moderate	fall	indoor	9
Men's Track	55	Moderate	both	both	10
Men's Basketball	19	High	both	indoor	11
Men's Swimming	38	Low	both	indoor	11
Women's Lacrosse	30	Moderate	spring	outdoor	12
Women's Soccer	35	High	fall	outdoor	13
Women's Track	55	Moderate	both	both	13
Baseball	48	Moderate	spring	outdoor	14
Men's Lacrosse	43	Moderate	spring	outdoor	17
Men's Wrestling	40	High	both	indoor	23
Football	95	High	fall	outdoor	48

Number of students, contact level (as determined via standardized definitions in **Appendix Table 3**), season, location, and number of COVID-19 cases per sports team. Teams with fewer than 5 cases were labeled as "< 5" to minimize the risk of de-anonymity. Teams are sorted by number of COVID-19 cases, then by contact level.

Appendix Table 3

Appendix Table 3. Sports contact level definitions.

Contact level	Definition	CMU teams
Low	Individual or small group sports where contact within six feet of other participants can be avoided. Sports that can be conducted with social distancing, consistent wearing of face coverings when within six feet of other people, or individually with no sharing of equipment or the ability to clean the equipment between use by competitors.	Cross country, cycling, golf, swimming, tennis, triathlon, volleyball (club)

Moderate	Team sports that can be played with only incidental or intermittent close contact between participants. This category may also include sports that involve close, sustained contact, but with protective equipment in place that may reduce the likelihood of respiratory particle transmission between participants OR sports where social distancing is possible but that use equipment that can't be cleaned between participants.	Baseball, cheerleading, lacrosse, track, volleyball (sand, indoor)
High	Team sports with frequent or sustained close contact (and in many cases, face-to-face contact) between participants and high probability that respiratory particles will be transmitted between participants.	Basketball, football, soccer, wrestling

Definitions of contact levels for sports teams. Sports teams were assigned a contact level of low, medium, or high based on variables that affect transmission risk, including physical proximity and the use of face coverings. Contact-level categories were created by synthesizing risk profiles defined from the California Department of Health's "Outdoor and Indoor Youth and Recreational Adult Sports" communication in April 2021 and the Colorado High School Activities Association 2020-2021 sports risk profiles.

Appendix Table 4

Appendix Table 4. Chi-square analyses.

Variable	Chi-Square Statistic (df)	P-value (Uncorrected)
Class years (Fall 2020)	95.67 (5)	4.31×10^{-19}
Class years (Spring 2021)	296.95 (5)	4.54×10^{-62}
Sports contact level	36.59 (2)	1.13×10^{-8}
Sports location (indoor *vs.* outdoor)	1.60 (1)	0.21
Sports season	10.22 (2)	0.006
Sports teams	75.08 (25)	6.60×10^{-7}
Residence halls	31.30 (11)	9.87×10^{-4}

Results of Pearson's chi-squared test for categorical variables assessed for COVID-19 disease risk. Test statistics, degrees of freedom, and uncorrected p-values are reported.

Appendix Table 5

Appendix Table 5. Published viral genomic data for clinical and environmental specimens

Sequence Identifier (clinical)	Biosample Accession	GenBank Accession	GISAID Identifier	SRA Accession
USA/CO-Broad-CMU_00017/2020	SAMN17211059	MW521521	EPI_ISL_872745	SRS8145178
USA/CO-Broad-CMU_00039/2020	SAMN17211081	MW521525	EPI_ISL_872749	SRS8145099
USA/CO-Broad-CMU_00043/2020	SAMN17211085	MW521526	EPI_ISL_872750	SRS8145173
USA/CO-Broad-CMU_00051/2020	SAMN17211093	MW521527	EPI_ISL_872751	SRS8145098
USA/CO-Broad-CMU_00054/2020	SAMN17211096	MW521528	EPI_ISL_872752	SRS8145097
USA/CO-Broad-CMU_00060/2020	SAMN17211102	MW521529	EPI_ISL_872753	SRS8145065
USA/CO-Broad-CMU_00062/2020	SAMN17211104	MW521530	EPI_ISL_872754	SRS8145064

USA/CO-Broad-CMU_00063/2020	SAMN17211105	MW521531	EPI_ISL_872755	SRS8145063
USA/CO-Broad-CMU_00064/2020	SAMN17211106	MW521532	EPI_ISL_872756	SRS8145095
USA/CO-Broad-CMU_00073/2020	SAMN17211115	MW521533	EPI_ISL_872757	SRS8145059
USA/CO-Broad-CMU_00075/2020	SAMN17211117	MW521534	EPI_ISL_872758	SRS8145057
USA/CO-Broad-CMU_00079/2020	SAMN17211121	MW521535	EPI_ISL_872759	SRS8145055
USA/CO-Broad-CMU_00080/2020	SAMN17211122	MW521536	EPI_ISL_872760	SRS8145054
USA/CO-Broad-CMU_00084/2020	SAMN17211126	MW521537	EPI_ISL_872761	SRS8145052
USA/CO-Broad-CMU_00088/2020	SAMN17211130	MW521539	EPI_ISL_872763	SRS8145050
USA/CO-Broad-CMU_00089/2020	SAMN17211131	MW521540	EPI_ISL_872764	SRS8145049
USA/CO-Broad-CMU_00090/2020	SAMN17211132	MW521541	EPI_ISL_872765	SRS8145048
USA/CO-Broad-CMU_00091/2020	SAMN17211133	MW521542	EPI_ISL_872766	SRS8145166
USA/CO-Broad-CMU_00092/2020	SAMN17211134	MW521543	EPI_ISL_872767	SRS8145165
USA/CO-Broad-CMU_00094/2020	SAMN17211136	MW521544	EPI_ISL_872768	SRS8145046
USA/CO-Broad-CMU_00098/2020	SAMN17211140	MW521545	EPI_ISL_872769	SRS8145162
USA/CO-Broad-CMU_00100/2020	SAMN17211142	MW521546	EPI_ISL_872770	SRS8145160
USA/CO-Broad-CMU_00101/2020	SAMN17211143	MW521547	EPI_ISL_872771	SRS8145159
USA/CO-Broad-CMU_00103/2020	SAMN17211145	MW521548	EPI_ISL_872772	SRS8145157
USA/CO-Broad-CMU_00004/2020	SAMN17210672	MW454484	EPI_ISL_765574	pending
USA/CO-Broad-CMU_00007/2020	SAMN17210675	MW454485	EPI_ISL_765575	pending
USA/CO-Broad-CMU_00010/2020	SAMN17210678	MW454486	EPI_ISL_765576	pending
USA/CO-Broad-CMU_00107/2020	SAMN17211149	MW521549	EPI_ISL_872773	SRS8145044
USA/CO-Broad-CMU_00108/2020	SAMN17211150	MW521550	EPI_ISL_872774	SRS8145043
USA/CO-Broad-CMU_00109/2020	SAMN17211151	MW521551	EPI_ISL_872775	SRS8145155
USA/CO-Broad-CMU_00110/2020	SAMN17211152	MW521552	EPI_ISL_872776	SRS8145154
USA/CO-Broad-CMU_00111/2020	SAMN17211153	MW521553	EPI_ISL_872777	SRS8145093
USA/CO-Broad-CMU_00113/2020	SAMN17211155	MW454487	EPI_ISL_765577	pending
USA/CO-Broad-CMU_00114/2020	SAMN17211156	MW454488	EPI_ISL_765578	pending
USA/CO-Broad-CMU_00116/2020	SAMN17211158	MW454489	EPI_ISL_765579	pending
USA/CO-Broad-CMU_00118/2020	SAMN17211160	MW454490	EPI_ISL_765580	pending
USA/CO-Broad-CMU_00123/2020	SAMN17211165	MW454492	EPI_ISL_765582	pending
USA/CO-Broad_WarriorLab-00125/2021	SAMN17906199	MW617630	EPI_ISL_1011598	SRS8270659
USA/CO-Broad_WarriorLab-00126/2021	SAMN17906200	MW617631	EPI_ISL_1011599	SRS8270657
USA/CO-Broad_WarriorLab-00128/2021	SAMN17906202	MW617632	EPI_ISL_1011600	SRS8270660
USA/CO-Broad_WarriorLab-00130/2021	SAMN17906204	MW617633	EPI_ISL_1011601	SRS8270663
USA/CO-Broad_WarriorLab-00131/2021	SAMN17906205	MW617634	EPI_ISL_1011602	SRS8270664
USA/CO-Broad_WarriorLab-00132/2021	SAMN17906206	MW617635	EPI_ISL_1011603	SRS8270666
USA/CO-Broad_WarriorLab-00133/2021	SAMN17906207	MW617636	EPI_ISL_1011604	SRS8270665
USA/CO-Broad_WarriorLab-00134/2021	SAMN17906208	MW617637	EPI_ISL_1011605	SRS8270667
USA/CO-Broad_WarriorLab-00135/2021	SAMN17906209	MW617638	EPI_ISL_1011606	SRS8270668
USA/CO-Broad_WarriorLab-00136/2021	SAMN17906210	MW617639	EPI_ISL_1011607	SRS8270669
USA/CO-Broad_WarriorLab-00137/2021	SAMN17906211	MW617640	EPI_ISL_1011608	SRS8270670
USA/CO-Broad_WarriorLab-00138/2021	SAMN17906212	MW617641	EPI_ISL_1011609	SRS8270671
USA/CO-Broad_WarriorLab-00140/2021	SAMN17906214	MW617642	EPI_ISL_1011610	SRS8270675
USA/CO-Broad_WarriorLab-00141/2021	SAMN17906215	MW617643	EPI_ISL_1011611	SRS8270674
USA/CO-Broad_WarriorLab-00142/2021	SAMN17906216	MW617644	EPI_ISL_1011612	SRS8270676
USA/CO-Broad_WarriorLab-00145/2021	SAMN17906219	MW617645	EPI_ISL_1011613	SRS8270679
USA/CO-Broad_WarriorLab-00146/2021	SAMN17906220	MW617646	EPI_ISL_1011614	SRS8270680
USA/CO-Broad_WarriorLab-00147/2021	SAMN17906221	MW617647	EPI_ISL_1011615	SRS8270681
USA/CO-Broad_WarriorLab-00148/2021	SAMN17906222	MW617648	EPI_ISL_1011616	SRS8270682
USA/CO-Broad_WarriorLab-00187/2021	SAMN17906261	MW617679	EPI_ISL_1011647	SRS8270725
USA/CO-Broad_WarriorLab-00188/2021	SAMN17906262	MW617680	EPI_ISL_1011648	SRS8270724
USA/CO-Broad_WarriorLab-00189/2021	SAMN17906263	MW617681	EPI_ISL_1011649	SRS8270726
USA/CO-Broad_WarriorLab-00190/2021	SAMN17906264	MW617682	EPI_ISL_1011650	SRS8270727
USA/CO-Broad_WarriorLab-00191/2021	SAMN17906265	MW617683	EPI_ISL_1011651	SRS8270729
USA/CO-Broad_WarriorLab-00192/2021	SAMN17906266	MW617684	EPI_ISL_1011652	SRS8270731
USA/CO-Broad_WarriorLab-00162/2021	SAMN17906236	MW617658	EPI_ISL_1011626	SRS8270697
USA/CO-Broad_WarriorLab-00177/2021	SAMN17906251	MW617670	EPI_ISL_1011638	SRS8270711
USA/CO-Broad_WarriorLab-00178/2021	SAMN17906252	MW617671	EPI_ISL_1011639	SRS8270714
USA/CO-Broad_WarriorLab-00182/2021	SAMN17906256	MW617674	EPI_ISL_1011642	SRS8270719
USA/CO-Broad_WarriorLab-00149/2021	SAMN17906223	MW617649	EPI_ISL_1011617	SRS8270684
USA/CO-Broad_WarriorLab-00150/2021	SAMN17906224	MW617650	EPI_ISL_1011618	SRS8270685
USA/CO-Broad_WarriorLab-00151/2021	SAMN17906225	MW617651	EPI_ISL_1011619	SRS8270686

USA/CO-Broad_WarriorLab-00152/2021	SAMN17906226	MW617652	EPI_ISL_1011620	SRS8270687
USA/CO-Broad_WarriorLab-00153/2021	SAMN17906227	MW617653	EPI_ISL_1011621	SRS8270688
USA/CO-Broad_WarriorLab-00156/2021	SAMN17906230	MW617654	EPI_ISL_1011622	SRS8270691
USA/CO-Broad_WarriorLab-00157/2021	SAMN17906231	MW617655	EPI_ISL_1011623	SRS8270689
USA/CO-Broad_WarriorLab-00158/2021	SAMN17906232	MW617656	EPI_ISL_1011624	SRS8270692
USA/CO-Broad_WarriorLab-00163/2021	SAMN17906237	MW617659	EPI_ISL_1011627	SRS8270698
USA/CO-Broad_WarriorLab-00167/2021	SAMN17906241	MW617661	EPI_ISL_1011629	SRS8270701
USA/CO-Broad_WarriorLab-00168/2021	SAMN17906242	MW617662	EPI_ISL_1011630	SRS8270703
USA/CO-Broad_WarriorLab-00160/2021	SAMN17906234	MW617657	EPI_ISL_1011625	SRS8270695
USA/CO-Broad_WarriorLab-00169/2021	SAMN17906243	MW617663	EPI_ISL_1011631	SRS8270702
USA/CO-Broad_WarriorLab-00172/2021	SAMN17906246	MW617665	EPI_ISL_1011633	SRS8270708
USA/CO-Broad_WarriorLab-00173/2021	SAMN17906247	MW617666	EPI_ISL_1011634	SRS8270709
USA/CO-Broad_WarriorLab-00176/2021	SAMN17906250	MW617669	EPI_ISL_1011637	SRS8270713
USA/CO-Broad_WarriorLab-00179/2021	SAMN17906253	MW617672	EPI_ISL_1011640	SRS8270715
USA/CO-Broad_WarriorLab-00181/2021	SAMN17906255	MW617673	EPI_ISL_1011641	SRS8270717
USA/CO-Broad_WarriorLab-00183/2021	SAMN17906257	MW617675	EPI_ISL_1011643	SRS8270720
USA/CO-Broad_WarriorLab-00184/2021	SAMN17906258	MW617676	EPI_ISL_1011644	SRS8270722
USA/CO-Broad_WarriorLab-00185/2021	SAMN17906259	MW617677	EPI_ISL_1011645	SRS8270721
USA/CO-Broad_WarriorLab-00186/2021	SAMN17906260	MW617678	EPI_ISL_1011646	SRS8270723
USA/CO-Broad_WarriorLab-00193/2021	SAMN17906267	MW617685	EPI_ISL_1011653	SRS8270730
USA/CO-Broad_WarriorLab-00194/2021	SAMN17906268	MW617686	EPI_ISL_1011654	SRS8270732
USA/CO-Broad_WarriorLab-00195/2021	SAMN17906269	MW617687	EPI_ISL_1011655	SRS8270733
USA/CO-Broad_WarriorLab-00196/2021	SAMN17906270	MW617688	EPI_ISL_1011656	SRS8270734
USA/CO-Broad_WarriorLab-00197/2021	SAMN17906271	MW617689	EPI_ISL_1011657	SRS8270735
USA/CO-Broad_WarriorLab-00198/2021	SAMN17906272	MW617690	EPI_ISL_1011658	SRS8270736
USA/CO-Broad_WarriorLab-00199/2021	SAMN17906273	MW617691	EPI_ISL_1011659	SRS8270737
USA/CO-Broad_WarriorLab-00200/2021	SAMN17906274	MW617692	EPI_ISL_1011660	SRS8270739
USA/CO-Broad_WarriorLab-00201/2021	SAMN17906275	MW617693	EPI_ISL_1011661	SRS8270740
USA/CO-Broad_WarriorLab-00202/2021	SAMN17906276	MW617694	EPI_ISL_1011662	SRS8270741
USA/CO-Broad_WarriorLab-00203/2021	SAMN17906277	MW617695	EPI_ISL_1011663	SRS8270742
USA/CO-Broad_WarriorLab-00204/2021	SAMN17906278	MW617696	EPI_ISL_1011664	SRS8270744
USA/CO-Broad_WarriorLab-00205/2021	SAMN17906279	MW617697	EPI_ISL_1011665	SRS8270743
USA/CO-Broad_WarriorLab-00206/2021	SAMN17906280	MW617698	EPI_ISL_1011666	SRS8270745
USA/CO-Broad_WarriorLab-00207/2021	SAMN17906281	MW617699	EPI_ISL_1011667	SRS8270746
USA/CO-Broad_WarriorLab-00208/2021	SAMN17906282	MW617700	EPI_ISL_1011668	SRS8270747
USA/CO-Broad_WarriorLab-00209/2021	SAMN17906283	MW617701	EPI_ISL_1011669	SRS8270748
USA/CO-Broad_WarriorLab-00210/2021	SAMN17906284	MW617702	EPI_ISL_1011670	SRS8270749
USA/CO-Broad_WarriorLab-00211/2021	SAMN17906285	MW617703	EPI_ISL_1011671	SRS8270750
USA/CO-Broad_WarriorLab-00212/2021	SAMN17906286	MW617704	EPI_ISL_1011672	SRS8270752
USA/CO-Broad_WarriorLab-00213/2021	SAMN17906287	MW617705	EPI_ISL_1011673	SRS8270753
USA/CO-Broad_WarriorLab-00215/2021	SAMN17906289	MW617706	EPI_ISL_1011674	SRS8270754
USA/CO-Broad_WarriorLab-00216/2021	SAMN17906290	MW617707	EPI_ISL_1011675	SRS8270755
USA/CO-Broad_WarriorLab-00217/2021	SAMN17906291	MW617708	EPI_ISL_1011676	SRS8270756
USA/CO-Broad_WarriorLab-00218/2021	SAMN17906292	MW617709	EPI_ISL_1011677	SRS8270758
USA/CO-Broad_WarriorLab-00219/2021	SAMN18306824	MW749874	EPI_ISL_1253885	SRS8468532
USA/CO-Broad_WarriorLab-00220/2021	SAMN18306825	MW749875	EPI_ISL_1253886	SRS8468533
USA/CO-Broad_WarriorLab-00221/2021	SAMN18306826	MW749876	EPI_ISL_1253887	SRS8468534
USA/CO-Broad_WarriorLab-00222/2021	SAMN18306827	MW749877	EPI_ISL_1253888	SRS8468535
USA/CO-Broad_WarriorLab-00225/2021	SAMN18306830	MW749878	EPI_ISL_1253889	SRS8468539
USA/CO-Broad_WarriorLab-00226/2021	SAMN18306831	MW749879	EPI_ISL_1253890	SRS8468540
USA/CO-Broad_WarriorLab-00227/2021	SAMN18306832	MW749880	EPI_ISL_1253891	SRS8468541
USA/CO-Broad_WarriorLab-00228/2021	SAMN18306833	MW749881	EPI_ISL_1253892	SRS8468542
USA/CO-Broad_WarriorLab-00229/2021	SAMN18306834	MW749882	EPI_ISL_1253893	SRS8468543
USA/CO-Broad_WarriorLab-00230/2021	SAMN18306835	MW749883	EPI_ISL_1253894	SRS8468544
USA/CO-Broad_WarriorLab-00231/2021	SAMN18306836	MW749884	EPI_ISL_1253895	SRS8468545
USA/CO-Broad_WarriorLab-00287/2021	SAMN18306892	MW749928	EPI_ISL_1253939	SRS8468340
USA/CO-Broad_WarriorLab-00288/2021	SAMN18306893	MW749929	EPI_ISL_1253940	SRS8468257
USA/CO-Broad_WarriorLab-00232/2021	SAMN18306837	MW749885	EPI_ISL_1253896	SRS8468546
USA/CO-Broad_WarriorLab-00233/2021	SAMN18306838	MW749886	EPI_ISL_1253897	SRS8468547
USA/CO-Broad_WarriorLab-00234/2021	SAMN18306839	MW749887	EPI_ISL_1253898	SRS8468548
USA/CO-Broad_WarriorLab-00235/2021	SAMN18306840	MW749888	EPI_ISL_1253899	SRS8468551
USA/CO-Broad_WarriorLab-00236/2021	SAMN18306841	MW749889	EPI_ISL_1253900	SRS8468552

USA/CO-Broad_WarriorLab-00237/2021	SAMN18306842	MW749890	EPI_ISL_1253901	SRS8468386
USA/CO-Broad_WarriorLab-00239/2021	SAMN18306844	MW749891	EPI_ISL_1253902	SRS8468388
USA/CO-Broad_WarriorLab-00241/2021	SAMN18306846	MW749892	EPI_ISL_1253903	SRS8468390
USA/CO-Broad_WarriorLab-00242/2021	SAMN18306847	MW749893	EPI_ISL_1253904	SRS8468391
USA/CO-Broad_WarriorLab-00243/2021	SAMN18306848	MW749894	EPI_ISL_1253905	SRS8468392
USA/CO-Broad_WarriorLab-00244/2021	SAMN18306849	MW749895	EPI_ISL_1253906	SRS8468393
USA/CO-Broad_WarriorLab-00245/2021	SAMN18306850	MW749896	EPI_ISL_1253907	SRS8468395
USA/CO-Broad_WarriorLab-00246/2021	SAMN18306851	MW749897	EPI_ISL_1253908	SRS8468396
USA/CO-Broad_WarriorLab-00248/2021	SAMN18306853	MW749898	EPI_ISL_1253909	SRS8468398
USA/CO-Broad_WarriorLab-00249/2021	SAMN18306854	MW749899	EPI_ISL_1253910	SRS8468399
USA/CO-Broad_WarriorLab-00250/2021	SAMN18306855	MW749900	EPI_ISL_1253911	SRS8468400
USA/CO-Broad_WarriorLab-00251/2021	SAMN18306856	MW749901	EPI_ISL_1253912	SRS8468401
USA/CO-Broad_WarriorLab-00252/2021	SAMN18306857	MW749902	EPI_ISL_1253913	SRS8468402
USA/CO-Broad_WarriorLab-00253/2021	SAMN18306858	MW749903	EPI_ISL_1253914	SRS8468403
USA/CO-Broad_WarriorLab-00256/2021	SAMN18306861	MW749904	EPI_ISL_1253915	SRS8468407
USA/CO-Broad_WarriorLab-00257/2021	SAMN18306862	MW749905	EPI_ISL_1253916	SRS8468408
USA/CO-Broad_WarriorLab-00258/2021	SAMN18306863	MW749906	EPI_ISL_1253917	SRS8468409
USA/CO-Broad_WarriorLab-00260/2021	SAMN18306865	MW749907	EPI_ISL_1253918	SRS8468411
USA/CO-Broad_WarriorLab-00261/2021	SAMN18306866	MW749908	EPI_ISL_1253919	SRS8468412
USA/CO-Broad_WarriorLab-00262/2021	SAMN18306867	MW749909	EPI_ISL_1253920	SRS8468413
USA/CO-Broad_WarriorLab-00263/2021	SAMN18306868	MW749910	EPI_ISL_1253921	SRS8468313
USA/CO-Broad_WarriorLab-00264/2021	SAMN18306869	MW749911	EPI_ISL_1253922	SRS8468314
USA/CO-Broad_WarriorLab-00265/2021	SAMN18306870	MW749912	EPI_ISL_1253923	SRS8468316
USA/CO-Broad_WarriorLab-00266/2021	SAMN18306871	MW749913	EPI_ISL_1253924	SRS8468317
USA/CO-Broad_WarriorLab-00267/2021	SAMN18306872	MW749914	EPI_ISL_1253925	SRS8468318
USA/CO-Broad_WarriorLab-00268/2021	SAMN18306873	MW749915	EPI_ISL_1253926	SRS8468319
USA/CO-Broad_WarriorLab-00269/2021	SAMN18306874	MW749916	EPI_ISL_1253927	SRS8468320
USA/CO-Broad_WarriorLab-00271/2021	SAMN18306876	MW749917	EPI_ISL_1253928	SRS8468322
USA/CO-Broad_WarriorLab-00272/2021	SAMN18306877	MW749918	EPI_ISL_1253929	SRS8468323
USA/CO-Broad_WarriorLab-00273/2021	SAMN18306878	MW749919	EPI_ISL_1253930	SRS8468324
USA/CO-Broad_WarriorLab-00275/2021	SAMN18306880	MW749920	EPI_ISL_1253931	SRS8468327
USA/CO-Broad_WarriorLab-00282/2021	SAMN18306887	MW749923	EPI_ISL_1253934	SRS8468334
USA/CO-Broad_WarriorLab-00276/2021	SAMN18306881	MW749921	EPI_ISL_1253932	SRS8468328
USA/CO-Broad_WarriorLab-00278/2021	SAMN18306883	MW749922	EPI_ISL_1253933	SRS8468330
USA/CO-Broad_WarriorLab-00283/2021	SAMN18306888	MW749924	EPI_ISL_1253935	SRS8468335
USA/CO-Broad_WarriorLab-00284/2021	SAMN18306889	MW749925	EPI_ISL_1253936	SRS8468336
USA/CO-Broad_WarriorLab-00285/2021	SAMN18306890	MW749926	EPI_ISL_1253937	SRS8468338
USA/CO-Broad_WarriorLab-00286/2021	SAMN18306891	MW749927	EPI_ISL_1253938	SRS8468339
USA/CO-CDCBI-Warrior_00289/2021	SAMN18498486	MW834877	EPI_ISL_1413769	SRS8613058
USA/CO-CDCBI-Warrior_00290/2021	SAMN18498487	MW834878	EPI_ISL_1413771	SRS8613060
USA/CO-CDCBI-Warrior_00291/2021	SAMN18498488	MW834879	EPI_ISL_1413774	SRS8613059
USA/CO-CDCBI-Warrior_00292/2021	SAMN18498489	MW834880	EPI_ISL_1413776	SRS8613061
USA/CO-CDCBI-Warrior_00293/2021	SAMN18498490	MW834881	EPI_ISL_1413779	SRS8613063
USA/CO-CDCBI-Warrior_00294/2021	SAMN18498491	MW834882	EPI_ISL_1413781	SRS8613064
USA/CO-CDCBI-Warrior_00295/2021	SAMN18498492	MW834883	EPI_ISL_1413784	SRS8613065
USA/CO-CDCBI-Warrior_00296/2021	SAMN18498493	MW834884	EPI_ISL_1413787	SRS8613066
USA/CO-CDCBI-Warrior_00300/2021	SAMN18790465	MZ217780	EPI_ISL_2133621	SRS8763083
USA/CO-CDCBI-Warrior_00301/2021	SAMN18790466	MZ217781	EPI_ISL_2133623	SRS8763082
USA/CO-CDCBI-Warrior_00302/2021	SAMN18790467	MZ217782	EPI_ISL_2133625	SRS8763084
USA/CO-CDCBI-Warrior_00304/2021	SAMN18790469	MZ217783	EPI_ISL_2133626	SRS8763087
USA/CO-CDCBI-Warrior_00305/2021	SAMN18790470	MZ217784	EPI_ISL_2133628	SRS8763088
USA/CO-CDCBI-Warrior_00312/2021	SAMN19224119	MZ217786	EPI_ISL_2133928	SRS9003810
USA/CO-CDCBI-Warrior_00311/2021	SAMN19224118	MZ217785	EPI_ISL_2133927	SRS9003809
Sequence Identifier (wastewater)	**Biosample Accession**	**GenBank Accession**	**GISAID Identifier**	**SRA Accession**
USA-CO-Broad_CMU_W0011-2021	SAMN29048169			SRR19659512
USA-CO-Broad_CMU_W0012-2021	SAMN29048170			SRR19659511
USA-CO-Broad_CMU_W0013-2021	SAMN29048171			SRR19659500
USA-CO-Broad_CMU_W0014-2021	SAMN29048172			SRR19659489
USA-CO-Broad_CMU_W0015-2021	SAMN29048173			SRR19659478
USA-CO-Broad_CMU_W0016-2021	SAMN29048174			SRR19659475
USA-CO-Broad_CMU_W0017-2021	SAMN29048175			SRR19659474

USA-CO-Broad_CMU_W0018-2021	SAMN29048176			SRR19659473
USA-CO-Broad_CMU_W0019-2021	SAMN29048177			SRR19659472
USA-CO-Broad_CMU_W0020-2021	SAMN29048178			SRR19659471
USA-CO-Broad_CMU_W0021-2021	SAMN29048179			SRR19659510
USA-CO-Broad_CMU_W0030-2021	SAMN29048180			SRR19659509
USA-CO-Broad_CMU_W0034-2021	SAMN29048181			SRR19659508
USA-CO-Broad_CMU_W0040-2021	SAMN29048182			SRR19659507
USA-CO-Broad_CMU_W0043-2021	SAMN29048183			SRR19659506
USA-CO-Broad_CMU_W0082-2021	SAMN29048184			SRR19659505
USA-CO-Broad_CMU_W0084-2021	SAMN29048185			SRR19659504
USA-CO-Broad_CMU_W0094-2021	SAMN29048186			SRR19659503
USA-CO-Broad_CMU_W0095-2021	SAMN29048187			SRR19659502
USA-CO-Broad_CMU_W0109-2021	SAMN29048188			SRR19659501
USA-CO-Broad_CMU_W0130-2021	SAMN29048189			SRR19659499
USA-CO-Broad_CMU-W0031-2021	SAMN18858704			SRR19659498
USA-CO-Broad_CMU-W0033-2021	SAMN18858705			SRR19659497
USA-CO-Broad_CMU-W0035-2021	SAMN18858706			SRR19659496
USA-CO-Broad_CMU-W0038-2021	SAMN18858707			SRR19659495
USA-CO-Broad_CMU-W0039-2021	SAMN18858708			SRR19659494
USA-CO-Broad_CMU-W0042-2021	SAMN18858709			SRR19659493
USA-CO-Broad_CMU-W0044-2021	SAMN18858710			SRR19659492
USA-CO-Broad_CMU-W0045-2021	SAMN18858711			SRR19659491
USA-CO-Broad_CMU-W0046-2021	SAMN18858712			SRR19659490
USA-CO-Broad_CMU-W0047-2021	SAMN18858713			SRR19659488
USA-CO-Broad_CMU-W0053-2021	SAMN18858714			SRR19659487
USA-CO-Broad_CMU-W0054-2021	SAMN18858715			SRR19659486
USA-CO-Broad_CMU-W0058-2021	SAMN18858716			SRR19659485
USA-CO-Broad_CMU-W0059-2021	SAMN18858717			SRR19659484
USA-CO-Broad_CMU-W0062-2021	SAMN18858718			SRR19659483
USA-CO-Broad_CMU-W0069-2021	SAMN18858719			SRR19659482
USA-CO-Broad_CMU-W0070-2021	SAMN18858720			SRR19659481
USA-CO-Broad_CMU-W0101-2021	SAMN18858721			SRR19659480
USA-CO-Broad_CMU-W0107-2021	SAMN18858722			SRR19659479
USA-CO-Broad_CMU-W0108-2021	SAMN18858723			SRR19659477
USA-CO-Broad_CMU-W0127-2021	SAMN18858724			SRR19659476

Published sequences used in this study, listed with NCBI BioSample accessions, NCBI GenBank sequence accessions, GISAID identifiers, and/or SRA accessions.

Appendix Table 6

Appendix Table 6. Lineages present in sequenced wastewater samples

Sample ID	Date	Site	B.1.1.519	B.1.126	B.1.2	B.1.234	B.1.350	B.1.429	B.1.429.1	B.1.533
CO_CMU_W0011	2-12	Site 5			0.09				0.84	
CO_CMU_W0012	2-12	Site 5			0.11				0.84	
CO_CMU_W0013	2-12	Site 5			0.12				0.82	
CO_CMU_W0014	2-16	Site 1		1.00						
CO_CMU_W0015	2-16	Site 8			0.12			0.11	0.77	
CO_CMU_W0016	2-17	Site 3							1.00	

CO_CMU_W0017	2-17	Site 6			0.91					
CO_CMU_W0018	2-17	Site 7			1.00					
CO_CMU_W0019	2-17	Site 11								
CO_CMU_W0020	2-17	Site 4							1.00	
CO_CMU_W0021	2-17	Site 2			0.93					
CO_CMU_W0030	2-11	Site 6			0.13	0.31			0.54	
CO_CMU_W0034	2-15	Site 5			0.28				0.47	
CO_CMU_W0040	2-18	Site 11			0.79					
CO_CMU_W0043	2-18	Site 8						0.16	0.81	
CO_CMU_W0082	3-01	Site 6							0.93	
CO_CMU_W0084	3-01	Site 4			0.99					
CO_CMU_W0094	3-04	Site 5			0.58				0.34	
CO_CMU_W0095	3-04	Site 3			0.49				0.26	
CO_CMU_W0109	3-09	Site 1							1.00	
CO_CMU_W0130	3-18	Site 1							0.31	
CO_CMU_W0031	2-11	Site 1					0.03		0.96	
CO_CMU_W0033	2-15	Site 10							0.99	
CO_CMU_W0035	2-18	Site 5			0.99					
CO_CMU_W0038	2-18	Site 4			0.99					
CO_CMU_W0039	2-18	Site 1			0.93				0.05	
CO_CMU_W0042	2-18	Site 10							0.99	
CO_CMU_W0046	2-22	Site 4			0.99					
CO_CMU_W0058	2-23	Site 11			0.98					
CO_CMU_W0059	2-23	Site 5							0.85	
CO_CMU_W0062	2-23	Site 1							1.00	
CO_CMU_W0069	2-25	Site 5			0.99					
CO_CMU_W0070	2-25	Site 3							0.96	
CO_CMU_W0101	3-08	Site 3							0.99	
CO_CMU_W0107	3-08	Site 5							0.94	
CO_CMU_W0108	3-09	Site 3							0.99	
CO_CMU_W0127	3-16	Site 5	0.12		0.08				0.72	0.07

Wastewater-detected lineages and their relative abundances. For each wastewater sample, collection date and site of collection are also listed. Lineages and abundances were determined via application of the Freyja program, as described in detail in the Supplementary Methods.

Appendix Table 7

Appendix Table 7. Replicate-confirmed single nucleotide variant mutations identified in sequenced wastewater samples but not present in sequenced clinical samples

SNV	In CO	Change	Gene	Amino acid	Presence in proportion of 42 wastewater samples	Maximum allele frequency
T5260A	False	Synonymous	ORF1ab	T1665T	10%	29%
T6174G	False	Missense	ORF1ab	I1970S	17%	32%
T9843A	False	Stop	ORF1ab	L3193*	14%	4%
C10650T	False	Missense	ORF1ab	T3462I	31%	100%
T27444G	False	Synonymous	ORF7a	L17L	7%	27%
C835T	True	Synonymous	ORF1ab	F190F	38%	100%
C6501T	True	Missense	ORF1ab	P2079L	38%	99%
G14126A	True	Missense	ORF1ab	S4621N	5%	100%
C21952T	True	Synonymous	S	V130V	38%	100%
T26099C	True	Missense	ORF3a	I236T	33%	100%
C28344T	True	Missense	N	T24I	38%	96%

Replicate-confirmed mutations identified in wastewater samples from CMU, but not in clinical samples. SNV nucleotide changes and positions are listed in bp, relative to the reference ancestral genome, NC_045512.2 (1st column) along with corresponding amino acid changes (4th and 5th columns), the class of change (3rd column), the proportion of samples bearing the change (6th column), and the highest allele frequency of that change amongst those samples (final column). Some of these mutations were present in Colorado clinical viral genomes (2nd column), or representative of specific Pango lineages (penultimate column).

Appendix Table 8

Appendix Table 8. Nucleotide and amino acid substitutions present in the B.1.429.1 lineage

Region	Amino Acid Changes Characteristic of B.1.429	Additional Amino Acid Changes Characteristic of B.1.429.1
ORF1a	T265I, I4205V	F2827L, V3367I
ORF1b	P314L, D1183Y	P314L, D1183Y
S	S13I, W152C*, L452R*, D614G*	Q677H

ORF3a	Q57H	A23V
N	T205I*	P142S, M234I*
ORF8		V100L

Characteristic amino acid mutations for B.1.429.1 and parent lineage B.1.429. Mutations are categorized by location / gene. Mutations with an accompanying asterisk were not seen in all B.1.429.1 sequenced genomes; however, this may have been due to gaps in sequencing coverage.

Appendix Table 9

Appendix Table 9. Summary of data sources used at Colorado Mesa University for their infectious disease surveillance program and additional recommendations for future institutional surveillance programs.

	Epidemiological Analyses	**Clinical Viral Genomic Sequencing**	**Wastewater Surveillance & Sequencing**	**Wifi Proximity Analyses**
General Utility	Identify epidemiological risk factors	Parametrize cluster distribution and identify lineages and mutations	Establish quality control standards	Discriminate interaction patterns by test positivity
Current Utility to Institution	Specify athletic, residential, and class-year risks	Identify VoC/VoI & transmission clusters	Designate testing resources based on surveillance; sequencing to detect mutations not seen clinically	———————
Potential for Future Utility	Automatically integrate metadata, wastewater surveillance, sequencing, and wifi-based contact tracing into comprehensive surveillance system made directly accessible for the community or public health officials			
Cost of Acquisition	*Medium*: Personnel (cataloging information)	*Medium*: Transportation of excess clinical samples	*Medium–High*: Establishment of collection devices	*Low*: Established infrastructure
Cost of Analysis	*Low*: Personnel (analysis)	*High*: Sequencing reagents and computing resources	*Low*: PCR reagents *Medium*: Sequencing costs reduced relative to clinical due to fewer samples	*Low*: Computing resources
Difficulty of Analysis	*Low*: Established statistical methods	*Low*: Established tools for phylogenetic trees	*Low*: Established tools for PCR analysis	*High*: Few established tools

			Medium: Few established tools/methods for mixed sequence analysis	

Comparison of the utility and costs of each data source utilized in this study. We recommend incorporation of these tools in a specific manner given resource availability (Figure 7). VoC = Variant of Concern; VOI = Variant of Interest.

Appendix Table 10

Appendix Table 10. Jaccard similarity between clusters derived from genomic reconstruction supplemented by different contact tracing data sets

Comparison Groups	Cluster Color	Jaccard Similarity
CT *vs.* 2-Day Wifi	Orange	.421
	Light Blue	1.0
	Pink	0.0
	Yellow	1.0
CT *vs.* 10-Day Wifi	Orange	.889
	Light Blue	1.0
	Pink	1.0
	Yellow	1.0
2-Day Wifi *vs.* 10-Day Wifi	Orange	.474
	Light Blue	1.0
	Pink	0
	Yellow	1.0

We computed the Jaccard similarity for distinct transmission reconstruction networks for individuals with the B.1.429.1 lineage. We supplemented the genomic reconstruction in the trials using three different definitions of close contacts: (1) manual contact tracing data, (2) 10-day wifi-derived contacts, and (3) 2-day wifi-derived contacts.

Appendix Table 11

Appendix Table 11. Summary of metrics used for the wifi proximity network analyses

Metric Name	Variables	Formula and Text Description	Figure Panel

(Median of) Daily Contacts	*individual*	$Median\left\{\begin{matrix}\text{for each day present on campus:}\\ \text{number of unique contacts for } individual\end{matrix}\right\}$ For each day that an individual is present on campus, calculate number of unique contacts; then take the median.	Figure 3A, left
(Median of) Average Exposure Time per Contact	*individual*	$Median\left\{\begin{matrix}\text{for each day present on campus:}\\ \frac{\sum_{\text{unique contacts}} \text{total interaction time with } individual}{\text{number of unique contacts for } individual}\end{matrix}\right\}$ For each day than an individual is present on campus, calculate the total time spent with all contacts and the number of unique contacts. Divide the total time by the number of contacts per day and take the median of these values.	Figure 3A, right
Number of Days on Campus	*individual*	# of days that *individual* is connected to an AP Calculate the number of days an individual is present on campus.	Appendix Figure 5AB; Appendix Figure 7B
Number of Individuals on Campus	*day, user category*	# of individuals of *user category* connected to an AP on *day* For a given day, calculate the number of unique individuals of a given user category (i.e. semester positive vs semester negative) that are present on campus.	Appendix Figure 5CD, left
Proportion of Individuals on Campus	*day, user category*	$\frac{\#\text{ of individuals of } user\ category \text{ connected to an AP on } day}{Max\left\{\begin{matrix}\text{for each day:}\\ \#\text{ of individuals of } user\ category \text{ connected to an AP}\end{matrix}\right\}}$ For a given day, calculate the number of users of a given user category (i.e., semester positive or semester negative) present on campus. Divide by the maximum value of this metric for the given user category across all days.	Appendix Figure 5CD, right
(Median of) Median Duration of AP Connections	*day of week, building category*	$Median\left\{\begin{matrix}\text{for each day} \in day\ of\ week:\\ Median\left\{\begin{matrix}\text{for each AP connection} \in\ building\ category:\\ \text{duration of connection}\end{matrix}\right\}\end{matrix}\right\}$ For a given building type and a given day of the week (i.e., Monday), calculate the median AP connection duration for each day; then take the median. Building type can be 'all', 'residential', 'other', or 'academic'.	Appendix Figure 6AB
(Median of) Daily Number of AP Connections	*day of week, building category*	$Median\left\{\begin{matrix}\text{for each day} \in day\ of\ week:\\ \#\text{number of AP connections} \in building\ category\end{matrix}\right\}$ For a given building type and a given day of the week (i.e., Monday), calculate the total number of AP connections for each day; then take the median. Building type can be 'all', 'residential', 'other', or 'academic'.	Appendix Figure 6CD
Total Daily Interaction Duration	*pair, day*	$\sum_{\text{all interactions of } pair \text{ on } day} \text{interaction duration}$	Appendix Figure 7C; Appendix Figure 12A

		Across all interactions for a given pair on a given day, calculate the total contact time between the pair. Pairs are defined as two individuals connecting to the same access point at the same time.	
Median Daily Interaction Duration	*pair, day*	$Median\{\text{for each interaction of } pair \text{ on } day: \text{interaction duration}\}$ Across all interactions for a given pair on a given day, calculate the median contact time between the pair. Pairs are defined as two individuals connecting to the same access point at the same time.	Appendix Figure 7D; Appendix Figure 12B

The metric names, associated variables, formulas, text descriptions, and the associated figure panel are listed for all metrics used in wifi proximity network analyses.